This article is a *Plant Cell* Advance Online Publication. The date of its first appearance online is the official date of publication. The article has been edited and the authors have corrected proofs, but minor changes could be made before the final version is published. Posting this version online reduces the time to publication by several weeks.

Differential Recruitment of *WOX* Transcription Factors for Lateral Development and Organ Fusion in Petunia and *Arabidopsis* [W]

Michiel Vandenbussche,[a,1] Anneke Horstman,[a] Jan Zethof,[a] Ronald Koes,[b] Anneke S. Rijpkema,[a] and Tom Gerats[a]

[a] Department of Plant Genetics, Institute for Water and Wetland Research, Radboud University Nijmegen, 6525 ED, Nijmegen, The Netherlands

[b] Department of Genetics, Vrije Universiteit Amsterdam, 1081 HV Amsterdam, The Netherlands

Petal fusion in petunia (*Petunia* × *hybrida*) results from lateral expansion of the five initially separate petal primordia, forming a ring-like primordium that determines further development. Here, we show that *MAEWEST* (*MAW*) and *CHORIPETALA SUZANNE* (*CHSU*) are required for petal and carpel fusion, as well as for lateral outgrowth of the leaf blade. Morphological and molecular analysis of *maw* and *maw chsu* double mutants suggest that polarity defects along the adaxial/abaxial axis contribute to the observed reduced lateral outgrowth of organ primordia. We show that *MAW* encodes a member of the *WOX* (*WUSCHEL*-related homeobox) transcription factor family and that a partly similar function is redundantly encoded by *WOX1* and *PRESSED FLOWER* (*PRS*) in *Arabidopsis thaliana*, indicating a conserved role for *MAW*/*WOX1*/*PRS* genes in regulating lateral organ development. Comparison of petunia *maw* and *Arabidopsis wox1 prs* phenotypes suggests differential recruitment of *WOX* gene function depending on organ type and species. Our comparative data together with previous reports on *WOX* gene function in different species identify the *WOX* gene family as highly dynamic and, therefore, an attractive subject for future evo-devo studies.

INTRODUCTION

Evolution has generated a tremendous variation in reproductive structures within the plant kingdom. This ranges from flowerless spore-producing ferns and plants bearing simple, wind-pollinated flowers to highly specialized flower types exhibiting unique interactions with specific animals acting as pollinators. The evolutionary invention of petals, the usually brightly colored organs of the flower, is generally believed to have played a major role in the evolution of pollination syndromes. In many taxa throughout the angiosperms, petals fuse partly or completely to form a tubular structure, thereby creating a protective barrier enclosing the reproductive organs and nectaries in the center of the flower.

The genus *Petunia* belongs to the Solanaceae, in which petal fusion (sympetaly) is a common characteristic. Variations in petal tube length and diameter within the genus *Petunia* have been associated with distinct pollinators (Wijsman, 1983; Ando et al., 2001; Stuurman et al., 2004; Hoballah et al., 2007), suggesting that sympetaly may have evolved as an important component of pollination syndromes. Sympetaly in petunia (*Petunia* × *hybrida)* results from a prolonged lateral expansion of each of its five initially separate emerging petal primordia until they unite to form a ring-like primordium, determining further fused development. To gain insight into this process, we have analyzed two recessive mutants called *maewest* (*maw*) and *choripetala suzanne* (*chsu*), in which petal fusion is partly disrupted. Leaf and pistil development are also affected in *maw* and *chsu* mutants, indicating that *MAW* and *CHSU* play a more general role in organ development.

We further present the molecular analysis of *MAW* and show that *MAW* encodes a member of the *WOX* (*WUSCHEL*-like homeobox) family of homeobox transcription factors, of which 15 members have been identified in the *Arabidopsis thaliana* genome (Mayer et al., 1998; Haecker et al., 2004). All *Arabidopsis WOX* members characterized up to now are involved in regulating diverse aspects of development. *WUSCHEL*, the founding member of the family (Mayer et al., 1998), and the orthologs *TERMINATOR* from petunia (Stuurman et al., 2002) and *ROSULATA* from *Antirrhinum majus* (Kieffer et al., 2006) are required for maintenance of the stem cell population in the shoot. More recently, it was shown that *WOX5* performs a similar function in the root apical meristem and that *WOX5* and *WUS* are functionally equivalent (Sarkar et al., 2007). *WOX6*/*PRETTY FEW SEEDS2* (*PFS2*) is involved in ovule development (Park et al., 2005), while *PRESSED FLOWER* (*PRS*)/*WOX3* is required for the development of lateral sepals and stamens in the flower and of the stipules at the leaf base (Matsumoto and Okada, 2001; Nardmann et al., 2004). The expression pattern of several other *WOX* genes in *Arabidopsis* indicated a role for these in embryonic patterning (Haecker et al., 2004). For example, *WOX2* and *WOX8*/*STPL* act as complementary cell fate regulators in the apical and basal lineage, respectively, of the early proembryo (Haecker et al., 2004; Wu et al., 2007; Breuninger et al., 2008),

[1] Address correspondence to m.vandenbussche@science.ru.nl.
The author responsible for distribution of materials integral to the findings presented in this article in accordance with the policy described in the Instructions for Authors (www.plantcell.org) is: Michiel Vandenbussche (m.vandenbussche@science.ru.nl).
[W] Online version contains Web-only data.
www.plantcell.org/cgi/doi/10.1105/tpc.109.065862

while *WOX9*/*STIMPY* regulates early embryonic growth (Wu et al., 2007; Breuninger et al., 2008) but is also required for growth and maintenance of the shoot apical meristem, partly by positively regulating *WUS* expression (Wu et al., 2005). In petunia, it was recently shown that the *WOX8*/*9* homolog *EVERGREEN* is required for the cymose branching pattern of the petunia inflorescence (Rebocho et al., 2008). Finally, in *Arabidopsis*, an analysis of *WOX13* and *WOX14* suggests roles for these proteins in floral transition, with additional functions in root development and anther differentiation for *WOX14* (Deveaux et al., 2008).

To provide further evidence for the involvement of *WOX* genes in lateral organ development and to investigate the extent of functional conservation between *WOX* orthologs of different species, we aimed to analyze mutants of putative *Arabidopsis MAW* orthologs. Using a combined phylogenetic and structural analysis of the WOX family, we identified *Arabidopsis WOX1* as the closest homolog to petunia *MAW*. In contrast with *maw*, *wox1* null mutants did not display obvious developmental defects, suggesting that *WOX1* functions redundantly. We therefore searched for other *WOX* gene candidates that might obscure the function of *WOX1* in *Arabidopsis*.

Interestingly in this respect, it was shown that *ns1 ns2* (for *narrow sheath*) mutants in maize (*Zea mays*) display a reduction of the leaf blade (Nardmann et al., 2004) reminiscent of the *maw* leaf phenotype. However, *NS1* and *NS2* belong to the *PRS*/*WOX3* subfamily rather than to the *WOX1* subfamily. Despite the strong leaf phenotype of *ns* mutants in maize, leaf development is affected only in the lack of stipules in *Arabidopsis prs* null mutants, although *PRS* is expressed in the margins of developing leaves (Matsumoto and Okada, 2001; Nardmann et al., 2004).

The partially similar leaf phenotypes of petunia *maw* (*WOX1* subfamily) and maize *ns* mutants (*PRS*/*NS* subfamily) and the absence of such leaf phenotypes in both *Arabidopsis wox1* and *prs* single mutants indicated a possible overlap in function between *WOX1* and *PRS* subfamily members in *Arabidopsis*. Consistent with this hypothesis, we found that *wox1 prs* double mutants display a leaf phenotype comparable to *maw* in petunia, indicating a conserved role for *MAW*/*WOX1*/*PRS* genes in regulating lateral organ development.

We discuss how differences in *WOX* function and phylogeny in the different model species petunia, *Arabidopsis*, and maize may explain the deviating phenotypes of the respective orthologous single mutants.

RESULTS

Morphological Analysis of *maw* Mutants

Lateral outgrowth of the leaf blade in *maw* mutants is severely reduced (Figures 1A to 1C). In wild-type leaves, the palisade parenchyma (adaxial) and spongy parenchyma (abaxial) occupy roughly equal domains; they join at the divide of the margin (Figure 1E). In *maw* mutants, leaf margins are clearly thickened (Figure 1D), the increase in size being due to the enlargement of the spongy parenchyma, while the size of the palisade parenchyma remains unchanged (Figure 1F). From early flower developmental stages onwards, the lateral expansion of the petal primordia is strongly reduced in *maw* mutants (Figures 1L to 1N) compared with the wild type (Figures 1G to 1I), resulting in a failure of the petal primordia to fuse properly. The fusion defects in petals are usually limited to the upper part (corolla), but occasionally extend to the base of the petal tube. The most severe defects can be seen at the distal ends of the petals, which exhibit a radial organization (Figure 1M). In addition, the flanks of these radial structures are covered with trichomes, which in the wild type are found exclusively on the abaxial sides of petals. In wild-type flowers, the pistil originates from two separate carpel primordia, which during development make contact, become flattened at the adaxial side, and fuse (Figures 1G to 1K). Pistils of *maw* flowers display carpel fusion defects, with phenotypes ranging from a partially split stigma (Figure 1O) to a complete split of stigma and style (Figure 1P). As a consequence, female fertility is strongly reduced in *maw* mutants, although seeds can be obtained from the occasional flowers with mildly affected pistils. Sepals display similar defects as observed in leaves and bracts and fail to fuse at their base (Figures 2G and 2I). No obvious developmental defects were observed in the stamens of *maw* flowers.

Morphological Analysis of *chsu* and *maw chsu* Double Mutants

Leaves of *chsu* mutants are more narrow compared with the wild type (Figure 2A), but unlike in *maw* mutants, leaf margins and palisade and spongy parenchyma develop normally (cf. Figure 2B with 1E). The choripetalous phenotype of *chsu* flowers can be easily distinguished from the *maw* phenotype, as lack of fusion between the petals usually occurs at two or three places only, while extending further to the base of the petal tube (Figure 2H). *chsu* carpel fusion defects exhibit a phenotypic variation comparable to that of *maw* pistils, ranging from a partially split stigma to a completely separated stigma and style (Figure 2D). In addition, the length of *chsu* pistils is reduced (Figure 2D).

In *maw chsu* double mutants (see Methods), lateral outgrowth of the leaf blade is further diminished compared with either of the single mutants (Figure 2A), and the partial abaxialization observed at the margins of *maw* leaves is strongly enhanced (Figure 2C): *maw chsu* leaves are composed mainly of abaxial spongy parenchyma, while the remaining adaxial palisade cells are further reduced in number and become disorganized (cf. Figure 2C with 1F). Frequently, *maw chsu* double mutants develop leaves with a radial structure, while a limited leaf blade outgrowth remains at the distal end (Figure 2E). In *maw chsu* flowers, petal fusion is completely eliminated, and petals develop as fully separate radial structures covered all over by trichomes (Figures 2F and 2J). Only late in development, a limited petal blade outgrowth occurs in the region that normally composes the corolla (Figure 2J). Carpel fusion defects in *maw chsu* pistils are also more pronounced and extend into the ovary, thereby exposing the ovules (Figure 2D). In summary, all defects found in *maw* or *chsu* single mutants are strongly enhanced in the double mutant, indicating that *MAW* and *CHSU* function together in lateral organ development.

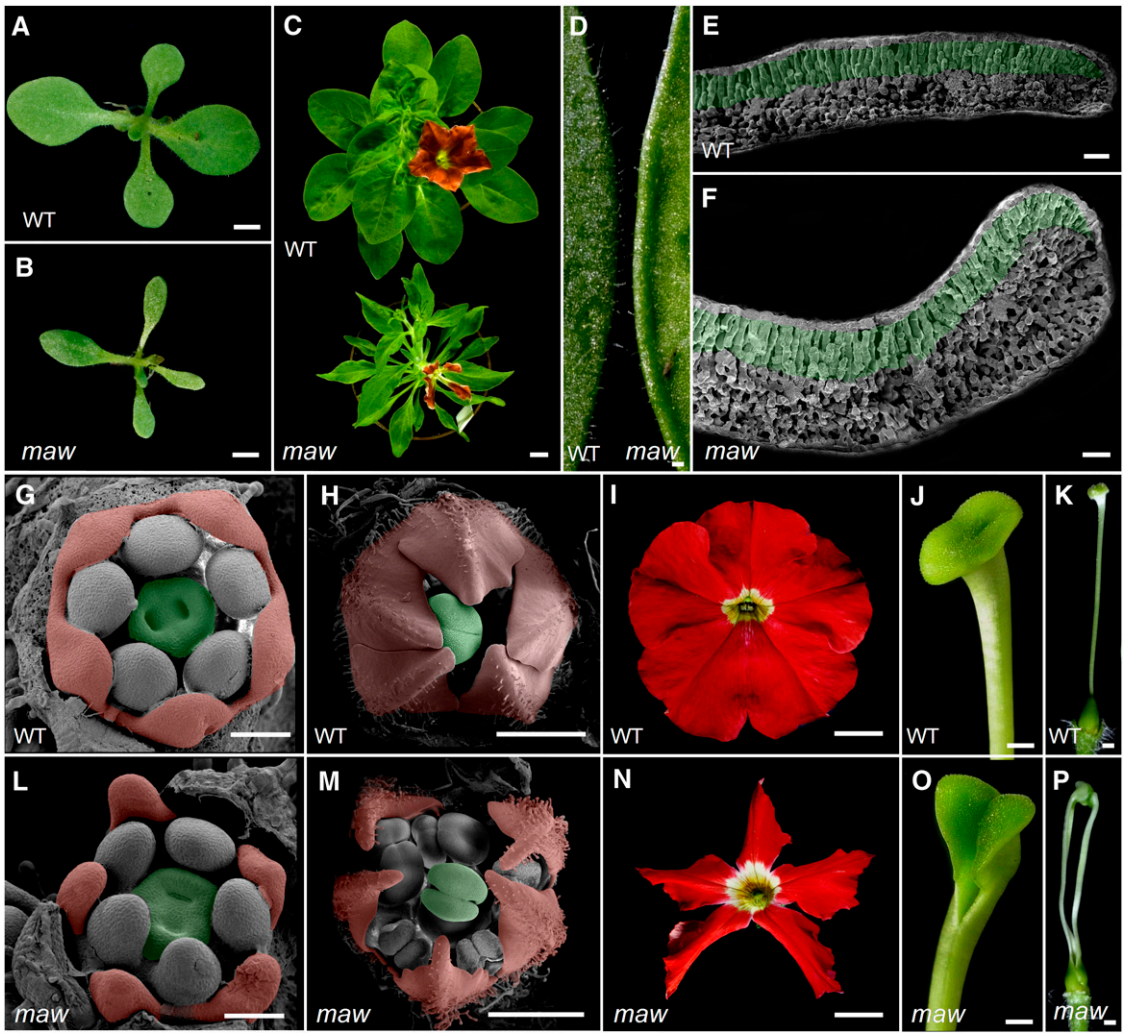

Figure 1. Phenotypic Analysis of Petunia *maw* Mutants.

(A) to **(F)** Vegetative phenotypes of petunia wild type and *maw* mutants at comparable stages of development.
(A) and **(B)** Seedlings.
(C) Top view of 7-week-old wild-type and *maw* plants with the first flower opening.
(D) Close-up of the leaf margins; note the thickened margins in *maw* leaves.
(E) and **(F)** Scanning electron microscopy images of freeze-fractured cross sections through wild-type and *maw* leaves. Adaxial palisade parenchyma tissue has been artificially colored in green.
(G) to **(P)** Flower phenotypes of petunia wild type and *maw* mutants at comparable stages of development.
(G), **(H)**, **(L)**, and **(M)** Scanning electron microscopy images of flower primordia. Sepals have been removed to reveal inner organization. Petal primordia are artificially colored in red and carpels in green.
(G) and **(L)** Stage in which carpel primordia start to emerge. Petal primordia are already flattened in the wild type and merge at their base. In *maw* mutants, lateral expansion of the petal primordia is reduced.
(H) and **(M)** Later stage showing the fusion of the two carpels in the wild type and the development of abaxial trichomes on the petal main veins. In *maw* mutants, carpels fail to fuse completely, while the distal ends of the petals are radial rather than flattened structures. Note the trichomes in these regions extending toward the adaxial side.
(I) and **(N)** Top view of fully developed flowers.
(J) and **(O)** Close-up of the pistil showing stigma.
(K) and **(P)** Entire pistils showing ovary, style, and stigma.
(O) A *maw* pistil with partially unfused carpels.
(P) A *maw* pistil with carpels unfused all the way down to the base of the ovary.
Bars = 2 mm in **(A)** and **(B)**, 1 cm in **(C)**, **(N)**, and **(I)**, 1 mm in **(D)**, **(H)**, **(K)**, **(M)**, and **(P)**, 0.5 mm in **(J)** and **(O)**, and 100 μm in **(E)** to **(G)** and **(L)**.

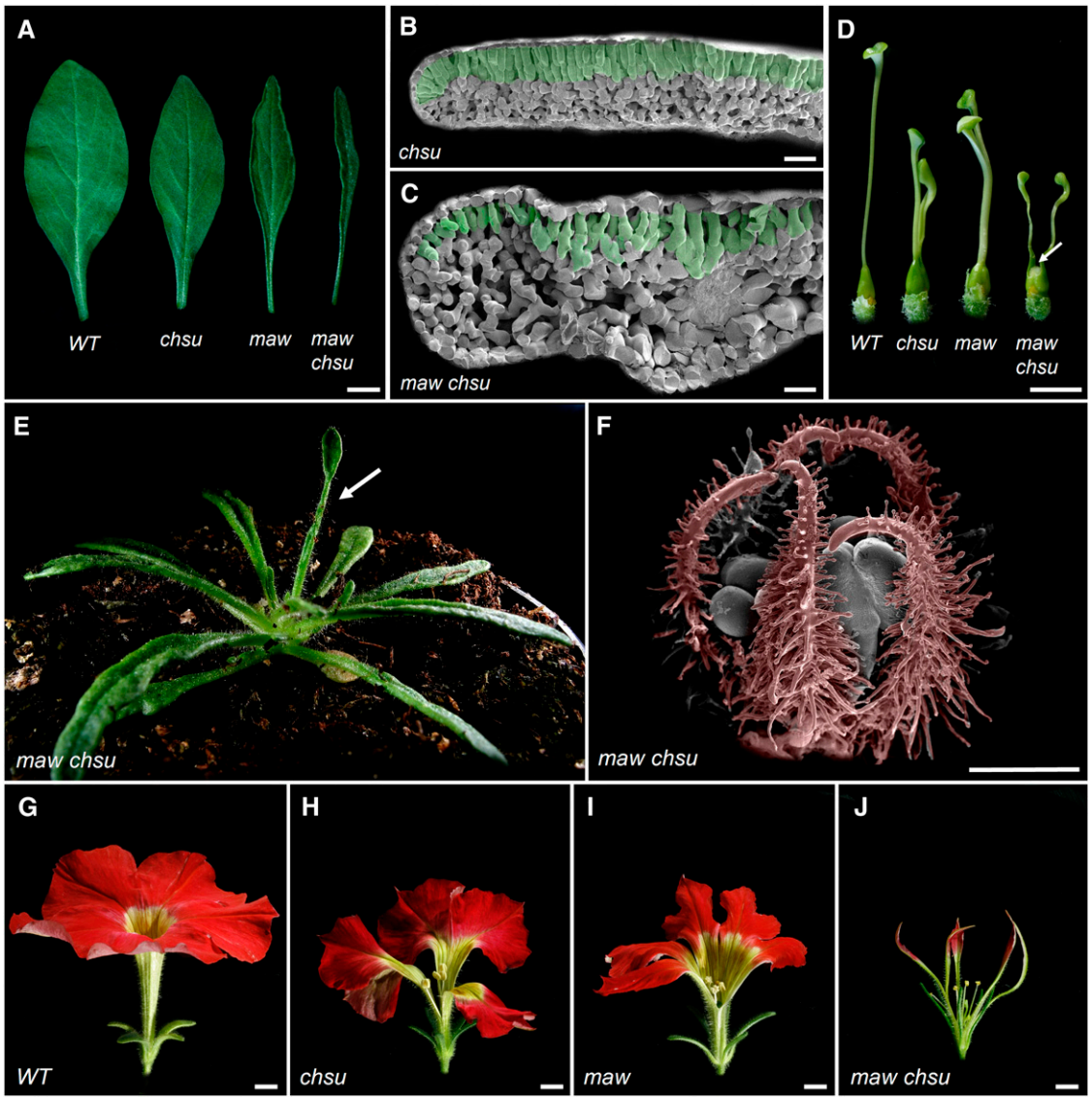

Figure 2. Phenotypic Analysis of Petunia *chsu* and *maw chsu* Double Mutants.

Genotypes are indicated in italics.
(A) Fully grown leaves of 5-week-old plants.
(B) and **(C)** Scanning electron microscopy images of freeze-fractured cross sections through fully grown leaves. Adaxial palisade parenchyma tissue has been artificially colored in green. Note the further reduction and disorganization of palisade parenchyma in **(C)**.
(D) Entire pistils showing fusion defects in mutant backgrounds and exposure of the ovules in *maw chsu* pistils (arrow).
(E) Rosette of a 4-week-old *maw chsu* mutant showing an almost completely radialized leaf (arrow).
(F) Scanning electron microscopy image of a *maw chsu* flower. Four of the five sepals have been removed to reveal inner organization. Petal primordia are artificially colored in red, and abaxial trichomes develop on all sides.
(G) to **(J)** Side view of fully grown flowers.
Bars = 1 cm in **(A)**, 100 μm in **(B)** and **(C)**, 5 mm in **(D)** and **(G)** to **(J)**, and 1 mm in **(F)**.

Molecular Characterization of *MAW*

We identified *maw* as a spontaneous recessive mutation segregating in a small family of the W138 petunia transposon line (Gerats et al., 1990). By transposon display (Van den Broeck et al., 1998), we identified a *dTph1* transposon that fully cosegregated with the original *maw-1* allele and that disrupts a gene encoding a homeodomain protein with high similarity to the *WOX* family of transcription factors (see Supplemental Figure 1 online) (Laux et al., 1996; Stuurman et al., 2002). To prove that the *maw* phenotype was caused by loss of function of this gene, we used a reverse genetics approach (Koes et al., 1995; Vandenbussche

et al., 2003b; Vandenbussche et al., 2008) to identify new insertion events in the gene. Two independent transposon insertion alleles were found (*maw-2*, first exon insertion; and *maw-3*, second exon insertion; Figure 3A), displaying similar phenotypes as *maw-1* when homozygous mutant. Crossing these mutants with *maw-1* demonstrated that the new insertions were allelic to *maw-1*. Furthermore, two additional *maw* alleles (*maw-4* and *maw-5*), which arose in independent populations, also contained *dTph1* insertions in the same gene. We therefore conclude that the observed phenotype is indeed caused by disruption of the *WOX* gene family member *MAW*.

The developmental defects seen in young emerging organ primordia of *maw* mutants (Figure 1) indicate that *MAW* is already active during the early stages of organ development. A quantitative RT-PCR experiment indeed showed that highest levels of *MAW* expression are found in the youngest tissues sampled (see Supplemental Figure 2 online). To examine the temporal and spatial *MAW* expression pattern in more detail, we performed in situ hybridization experiments. In young emerging bract and leaf primordia (Figures 3B and 3C), *MAW* expression is confined to a central narrow zone (arrows) corresponding to the provascular tissue. At the base of the bract primordium shown in Figure 3B, transcripts are detected in a broader region restricted to the adaxial side (asterisk). In further expanded leaves, expression is also found in a central zone (Figure 3C). In developing flower buds (Figure 3D), *MAW* transcripts are found in all emerging primordia. Expression in petals is localized centrally at the distal ends, while expression in stamen primordia is more uniformly distributed, as it is in the emerging carpel primordia. During later stages of flower development (Figure 3E), expression levels remain highest in the pistil, on the adaxial side of the two carpels where fusion occurs. Lower expression levels remain in a central zone and in the lateral margins of the petals and more uniformly distributed in the stamen loculi.

The presence of a homeodomain in MAW suggests a function as a transcriptional regulator. This is supported by the finding that a green fluorescent protein (GFP)-MAW fusion is targeted exclusively to the nucleus of tobacco (*Nicotiana tabacum*) BY-2 cells (Figure 3F).

Phylogenetic and Structural Analysis of the *WOX* Gene Family Identifies *WOX1* as the Putative *Arabidopsis MAW* Ortholog

To provide further evidence for the involvement of *WOX* genes in lateral organ development and to investigate the extent of functional conservation between *WOX* orthologs of different species, we aimed to analyze mutants of (a) putative *Arabidopsis MAW* ortholog(s). To identify these and to obtain more insight in the evolutionary relationship between members of the different subfamilies, we performed a combined structural and phylogenetic analysis of the *Arabidopsis* WOX family, including additionally isolated petunia members (see Methods), a selection of functionally characterized WOX proteins from other species, and all WOX proteins detected in the fully sequenced genomes of two additional eudicot species, grapevine (*Vitis vinifera*; Jaillon et al., 2007; Velasco et al., 2007) and poplar (*Populus* spp; http://genome.jgi-psf.org/), and of the two monocot species rice (Oryza sativa; International Rice Genome Sequencing Project, 2005) and sorghum (*Sorghum bicolor*; Paterson et al., 2009).

The neighbor-joining tree (Figure 4; see Supplemental Figure 4 online), based on the homeodomain region (see Supplemental Figure 3 online), and species distribution within the tree indicate the division of the family into different subfamilies with well-supported probabilities. These subfamilies can be classified further into large groups composed of either *WUS*/*WOX1-7*, *WOX8*, or *WOX13* homologs as described previously (Haecker et al., 2004; Deveaux et al., 2008). Because *MAW* belongs to the *WUS*/*WOX1-7* group, we analyzed this class in more detail first by comparing gene structure. In general, the number of exons within each subfamily defined by the tree architecture is strongly conserved but varies between the different subfamilies (Figure 4). In addition, we noticed the occurrence of several small peptide motifs that are specific to one or conserved between a few subfamilies only. Besides the previously identified WUS box (Haecker et al., 2004), we could identify small N-terminal (WOX1/4 subfamilies) and C-terminal motifs (all subfamilies) that are surprisingly well conserved within subfamilies, given the evolutionary distance between dicots and monocots (Figure 4). We named these conserved motifs after the subfamilies in which they are found, using *Arabidopsis* protein names as a reference (Figure 4). Thus, the obtained tree topology is fully supported both by the gene structure analysis and distribution of conserved peptide motifs.

According to this combined analysis, *MAW* is classified as a member of the *WOX1* subfamily, which harbors both *WOX1* and *PFS2*/*WOX6* genes from *Arabidopsis*. All *WOX1* members are encoded by four exons, while the other analyzed WUS/WOX1-7 subfamilies are encoded by either two or three exons (Figure 4). Notably, none of the monocot *WOX* genes classify into the *WOX1* subfamily, confirming previous studies (Nardmann and Werr, 2006; Nardmann et al., 2007). The tree topology identifies *WOX1* as the closest *Arabidopsis* relative to *MAW*, while *WOX6*/*PFS2* together with poplar *WOX6* are more distantly related members of the *WOX1* subfamily. This conclusion is also supported on the level of peptide motif conservation: in the first exon, we identified a motif called the 5′ WOX1/4 box, which is strongly conserved among *WOX1* and *WOX4* subfamily members, but is lacking in both *Arabidopsis* and poplar *WOX6* genes. Therefore, *WOX1* is the most likely *Arabidopsis WOX* gene candidate to encode a similar function as defined for *MAW*.

This conclusion is also consistent with the previously reported expression patterns of *WOX1* (Haecker et al., 2004; Nardmann et al., 2004) and *WOX6*/*PFS2* (Park et al., 2005). *WOX1* expression in developing embryos is confined to a central zone corresponding to the initiating vascular primordium of the cotyledons, similar to the expression of *MAW* in developing leaves and bracts. By contrast, *WOX6*/*PSF2* is most abundantly expressed in developing ovules but is also expressed in young leaf primordia, where transcripts are more uniformly distributed compared with *MAW* and *WOX1*.

The *wox1 prs* Double Mutant Displays a Phenotype Comparable to Petunia *maw*, Except for Pistil Development

To compare the function of the *Arabidopsis MAW* ortholog *WOX1* with petunia *MAW*, we analyzed four independent *wox1*

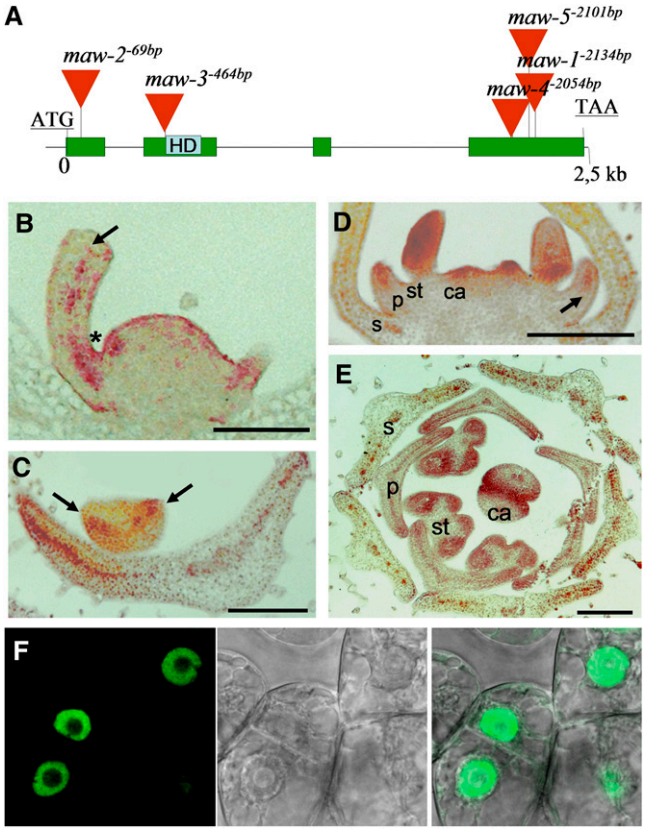

Figure 3. Cloning and Molecular Characterization of Petunia *MAW*.

(A) Genomic structure of the petunia *MAW* gene. Exons are represented by green boxes, introns by a single line, and *dTph1* transposon insertions by red triangles. Allele names are indicated with insert positions in superscript as number of base pairs downstream of the ATG start codon in the genomic sequence. Blue box marked with HD indicates the homeodomain.

(B) to **(E)** In situ localization of petunia *MAEWEST* transcripts in developing leaves and flower buds. Sections were hybridized with a digoxigenin-labeled antisense *MAW* RNA probe (red staining).

(B) and **(C)** *MAW* expression in vegetative organs (leaves and bracts).

(B) Longitudinal section through a meristem with an emerging bract primordium. Expression is localized to the adaxial side at the base of the emerging bract (asterisk) and, more distally, confined to a narrow stripe corresponding to the provascular tissue (arrow).

(C) Cross-section through developing leaves, including a young still round-shaped leaf stage and a further expanded leaf. Sections are oriented with the adaxial side above. *MAW* is detected in a central stripe in the youngest leaf cross section (arrows), and this pattern is maintained during later stages.

(D) and **(E)** *MAW* expression in developing flowers.

(D) Longitudinal section through a young flower bud with just emerging carpel primordia. At this stage, *MAW* transcripts are found central at the distal ends of emerging petal primordia (arrow) and more uniformly distributed in the developing stamens and emerging carpel primordia.

(E) Cross section through an almost fully developed flower bud sectioned at the height of the stigma. Strongest expression remains at the adaxial side of the carpels where fusion occurs, in the stamen loculi, and the margins of the petals. Identity of the floral organs in **(D)** and **(E)** are indicated as follows: s, sepal; p, petal; st, stamen; and ca, carpel. Bars = 200 μm in **(C)** to **(E)** and 100 μm in **(B)**.

transposon insertion lines from the ZIGIA collection (see Supplemental Figure 5 online). Two of these lines contain insertions disrupting the first exon and the homeodomain, respectively, and were therefore expected to represent full knockout alleles. However, we did not observe an obvious phenotype in homozygous mutants of these lines nor for the two homozygous intron insertion mutants (see Supplemental Figure 6 online). To further investigate this, we analyzed *WOX1* transcripts in *wox1* homozygous mutants (line 8AAJ85; see Supplemental Figure 5 online), showing complete absence of wild-type transcripts. This demonstrates that the *EN1* transposon is stably inserted and excludes the possibility that the absence of a clear phenotype in *wox1* mutants would be due to active excision of the *EN1* transposon. Together, this indicates that *WOX1* functions redundantly in *Arabidopsis*, in contrast with its ortholog in petunia.

Because *WOX6/PFS2* is the closest relative of *WOX1* (Figure 4), we tested if *WOX6/PFS2* might act redundantly with *WOX1* despite its divergent expression pattern, its reported function in ovule development (Park et al., 2004, 2005), and its divergent sequence characteristics (Figure 4). We could not observe a *maw*-like phenotype in *wox1 wox6/pfs2-2* mutants; leaves, sepals, petals, and carpels developed normally in the double mutants (see Supplemental Figures 5 and 6 online). This indicates that the absence of a *maw*-like phenotype in *wox1* single mutants cannot be explained by a functional redundancy of *WOX1* with *WOX6/PFS2*. Either *WOX1* plays a different role compared with *MAW* in petunia, or *WOX1* does encode a *maw*-like function but shares that function with a gene(s) other than *WOX6/PFS2.*

The observed leaf blade reduction in both petunia *maw* (*WOX1* subfamily) and maize *ns* mutants (*PRS* subfamily) and the absence of leaf phenotypes in both *Arabidopsis wox1 wox6* and *prs* mutants suggested a possible overlap in function between *WOX1* and *PRS* subfamily members in *Arabidopsis* (see Introduction). Consistent with this, we found that *WOX1* expression in leaf primordia overlaps with *PRS* in the lateral margins (see Supplemental Figure 5 online), similar to what we observed for *MAW* expression in young developing petunia leaves (cf. with Figure 3C, arrows).

To test the hypothesis of a functional overlap between *WOX1* and *PRS* genes, we crossed the obtained *wox1 wox6* double mutants with homozygous *prs* mutants. In all resulting F2 populations derived from these crosses, in addition to wild-type-appearing seedlings, seedlings were found at a frequency close to 1/16 (27/504) that displayed a reduction of the leaf blade in combination with thickened leaf margins, very reminiscent of the phenotype observed in petunia *maw* mutants (Figures 5A to 5C). A segregation analysis for *wox1*, *wox6*, and *prs* insertion alleles revealed that all phenotypically selected individuals with a *maw*-like phenotype were plants homozygous mutant for both *wox1* and *prs*, while all wild-type-appearing seedlings were genotyped

(F) Subcellular localization of the 35S:GFP-MAW construct in tobacco BY cells analyzed by confocal laser microscopy. Left, nuclear-localized GFP signal; middle, differential interference contrast image; right, merged image of GFP and differential interference contrast images.

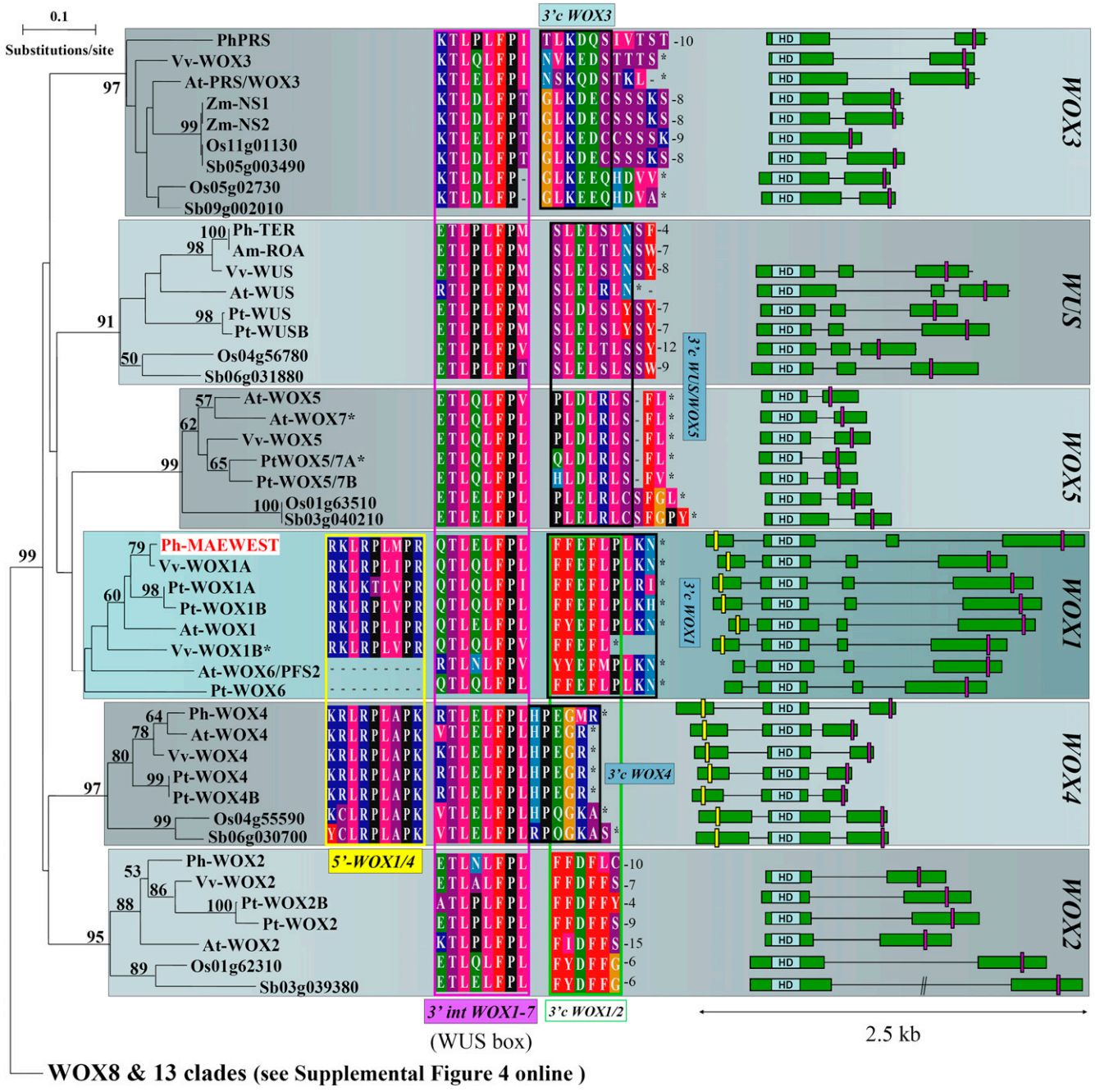

Figure 4. Phylogenetic and Structural Analysis of the *WOX* Gene Family.

For the neighbor-joining tree, 1000 bootstrap samples were generated to assess support for the inferred relationships. Local bootstrap probabilities are indicated near the branching points. Species names precede protein names and are abbreviated as follows: Vv, *Vitis vinifera*; At, *Arabidopsis thaliana*; Am, *Antirrhinum majus*; Ph, *Petunia hybrida*; Pt, *Populus trichocarpa*; Os, *Oryza sativa*; Sb, *Sorghum bicolor*; Zm, *Zea mays*. Accession codes are provided in Supplemental Table 2 online. An asterisk after the gene name indicates a deviating gene model compared with automatic predictions in the database. Short conserved peptide motifs are shown right from the tree and are named after their position relative to the homeodomain: 5′, upstream; 3′int, downstream internal; 3′c, C-terminal, combined with the name of subfamily(ies) for which they are diagnostic. Asterisks after C-terminal motifs represent stopcodons; in all other cases, the numbers after motifs indicate the number of remaining nonconserved amino acid residues before the stop codon is encountered. Exon/intron structures for members of the *WUS/WOX1-7* subclass are shown at the right. Exons are represented by green boxes and introns by black lines. HD, homeodomain region. Yellow and purple boxes indicate position of the 5′ WOX1/4 box and the 3′int WUS box, respectively.

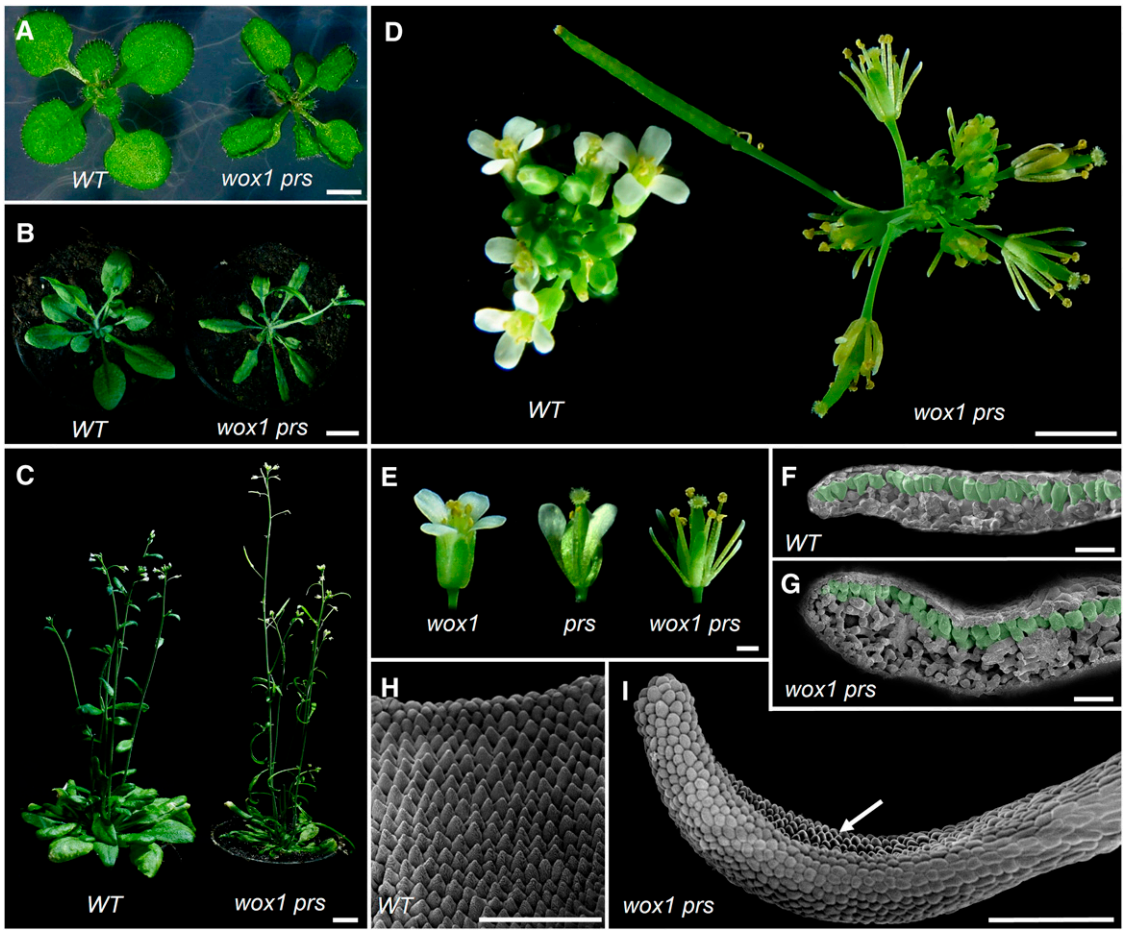

Figure 5. Leaf and Flower Phenotypes of *Arabidopsis* Wild-Type and *wox1 prs* Mutants.

Genotypes are indicated in italics below the images.
(A) Seedling stage.
(B) Rosette at the beginning of flowering.
(C) Flowering plants.
(D) Inflorescence top view.
(E) Side view of individual flowers.
(F) to **(I)** Scanning electron microscopy images.
(F) and **(G)** Freeze-fractured cross sections through wild-type and *wox1 prs* leaves. Adaxial palisade parenchyma tissue has been artificially colored in green.
(H) Epidermis of wild-type petals showing the typical conical petal cells at the adaxial side.
(I) *wox1 prs* petals showing the flattened abaxial petal epidermis cells extending to the adaxial side. A small group of normal conical cells remains in the middle (arrow).
Bars = 0.25 cm in **(A)** and **(D)**, 1 cm in **(B)** and **(C)**, 500 μm in **(E)**, and 100 μm in **(F)** to **(I)**.

as any of the other possible genotypes derived from a *wox1 wox6* x *prs* cross. Comparison of cross sections of the wild type (or any of the single mutants) with *wox1 prs* double mutant leaves revealed a similar increase in abaxial tissue as found in *maw* leaves (Figures 5F and 5G). In addition, flowers of *wox1 prs* mutants have very narrow petals (Figures 5D and 5E). Scanning electron microscopy analysis of these petals (Figures 5H and 5I) shows a radial-like organization at the distal ends, while flattened petal epidermal cells normally present only on the abaxial side, now extend beyond the leaf margin to the adaxial side with only a few of the typical adaxial conical petal cells remaining. In addition, all sepals are narrower, and the lateral petals are often missing or reduced as can be observed in single *prs* mutant flowers (Figure 5E). In contrast with petunia *maw* mutants, the fusion of the carpels and further pistil development and fertility are unaffected in *wox1 prs* double mutants (Figures 5D and 5E). Finally, the leaf and flower phenotype of the *wox1 wox6 prs* triple mutants was not distinguishable from that of *wox1 prs* double mutants (see Supplemental Figure 6 online), suggesting that *WOX6* is not involved in the same function(s). Nevertheless, we

cannot exclude that *WOX6* has an overlapping function with *WOX1* and *PRS* that remains hidden because of redundancy with yet another *WOX* subfamily member. Further analysis including other *WOX* (sub)family members should answer this question. In summary, the phenotype of *wox1 prs* mutants indicates that a *maw*-like function in *Arabidopsis* is encoded in a largely redundant fashion by *WOX1* and *PRS*.

Expression Analysis of Organ Polarity Determinants in *Arabidopsis* and Petunia Mutants

The proliferation of abaxial tissue at the leaf margins of petunia *maw* and *maw chsu* mutants and of *Arabidopsis wox1 prs* mutants suggests a defect in organ polarity regulation. In *Arabidopsis*, organ polarity regulation has been characterized extensively at the molecular level. We therefore have monitored the expression levels of a selection of *Arabidopsis* genes known to be involved in abaxial/adaxial patterning. The selection of genes comprises *FILAMENTOUS FLOWER/YABBY1* (*YAB1*) (Sawa et al., 1999; Siegfried et al., 1999; Eshed et al., 2004), *KANADI* (*KAN*) (Kerstetter et al., 2001; Emery et al., 2003; Wu et al., 2008), *AUXIN RESPONSE FACTOR4* (*ARF4*) and *ETTIN* (*ETT*) (Pekker et al., 2005) promoting abaxial cell fate, and *REVOLUTA* (Emery et al., 2003; Prigge et al., 2005), *ASYMMETRIC LEAVES1* (*AS1*) (Li et al., 2005; Garcia et al., 2006; Xu et al., 2006), *AS2* (Iwakawa et al., 2002; Lin et al., 2003), and the ribosomal gene *RPL28A* (Pinon et al., 2008; Yao et al., 2008) promoting adaxial identity. Wild-type and *wox1 prs* samples consisted of pooled shoot samples including emerging leaf primordia. None of the monitored *Arabidopsis* genes exhibited significant changes in transcript levels between *wox1 prs* mutant samples and the wild type, except for the *ARF4* gene, which was moderately upregulated in *wox1 prs* mutants (Figure 6A). Although only a subtle effect, upregulation of the abaxial cell fate–promoting *ARF4* gene is consistent with our morphological observations. The other ARF member *ETT* exhibited a similar upregulation, but with a low statistical significance. We identified petunia homologs of the set of *Arabidopsis* abaxial determinants and monitored their expression in the wild type, *maw*, *chsu*, and *maw chsu* double mutants (Figure 6B). In *maw* single mutants, *ARF4* and *ETT* homologs are upregulated to a similar degree as observed in *Arabidopsis wox1 prs* mutants but with a low statistical significance. In *chsu* mutants, the upregulation of *ARF4* and *ETT* homologs is more pronounced compared with *maw* mutants, whereas in *maw chsu* double mutants, the expression of the petunia *ARF4* and *ETT* homologs is further enhanced compared with the wild type and *maw* and *chsu* single mutants and is statistically well supported. In addition, a moderate upregulation of *KAN* homolog expression in *maw chsu* mutants also becomes statistically significant.

DISCUSSION

MAW and *CHSU* Are Required for Laminar Growth in Petunia, and *MAW* Encodes a Member of the *WOX1* Subfamily of WUSCHEL-Like Homeodomain Transcription Factors

To start to dissect the molecular basis of petal fusion in petunia, we analyzed *maw* and *chsu* mutants, in which petal fusion is disrupted. Morphological analysis shows that *maw* petals exhibit a reduced lateral development from early stages onwards, ultimately resulting in petal primordia that fail to fuse. Similar developmental defects were observed in leaves, bracts, and sepals and carpels, demonstrating that *MAW* plays a role in lateral development of plant organs in general. While petal and carpel fusion are also severely affected in *chsu* mutants, leaf blade outgrowth is only mildly diminished, and no dorsoventral patterning defects seem to occur at the leaf margins (Figure 2). Blade reduction of all organs is strongly enhanced in *maw chsu* double mutants (Figure 2), indicating that *MAW* and *CHSU* play overlapping roles in laminar growth. This is also supported by the similar downstream molecular effects observed in the single

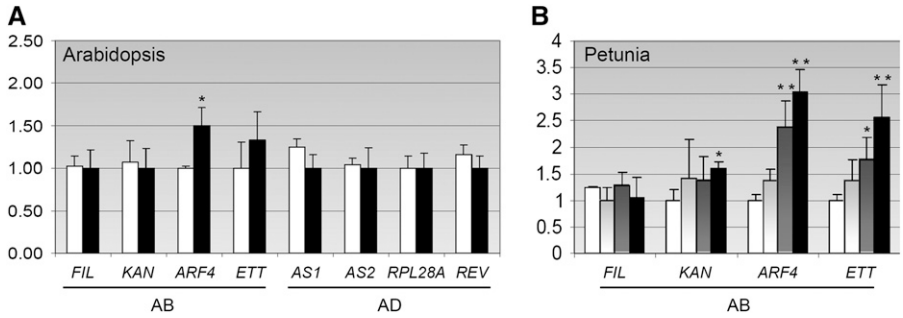

Figure 6. Organ Polarity Gene Expression Analysis in the Wild Type and Mutants by Quantitative RT-PCR.

The *y* axis shows x-fold expression with respect to the lowest encountered value equal to one. Error bars represent SD calculated from two technical replicates done on two biological replicates. Gene names of measured transcript levels are indicated below the bars.

(A) Expression levels in shoot samples, including leaf primordia of 2-week-old *Arabidopsis* wild type (white bars) and *wox1 prs* mutants (black bars).

(B) Expression levels in shoot samples, including leaf primordia of 30-d-old petunia wild type (white bars), *maw* mutants (light-gray bars), *chsu* mutants (dark-gray bars), and *maw chsu* mutants (black bars). AB, abaxial determinants; AD, adaxial determinants. Differential expression values between mutant and wild-type samples were tested for statistical significance (see Methods). Differences with a $P < 0.05$ (one asterisk), and $P < 0.001$ (two asterisks) resulting from a one-way analysis of variance test are indicated.

mutants (Figure 6) and enhancement thereof in the double mutants (see below).

While the identity of *CHSU* remains to be determined, we found that *MAW* encodes a member of the *WOX* family of homeobox transcription factors (Mayer et al., 1998; Haecker et al., 2004). To identify a putative *MAW* ortholog in *Arabidopsis* and to obtain a better insight into the evolutionary diversification of the *WOX* gene family, we combined a phylogenetic analysis with a structural analysis. WOX proteins belonging to different subfamilies in general display very low sequence similarity outside of the highly conserved homeodomain region. Phylogenetic reconstructions of the complete WOX family are therefore restricted to this region, which unfortunately does not contain sufficient information to resolve evolutionary relationships between different subfamilies. As a consequence, WOX trees are obtained displaying poorly supported bootstrap values between subfamilies (Figure 4; Haecker et al., 2004; Nardmann and Werr, 2006; Nardmann et al., 2007). We tried to overcome this problem by combining the tree topology with data on exon/intron structures and the detection of small conserved peptide motifs that are diagnostic for specific subfamilies (Deveaux et al., 2008). Such signatures have proven already useful to understand better the evolution of other transcription factor families (e.g., Vandenbussche et al., 2003a; Jiang et al., 2004) and can enhance the accuracy of gene structure and function prediction (see Supplemental Table 2 online).

Haecker et al. (2004) previously identified in WUS orthologs and in *Arabidopsis* WOX1-7 proteins a short motif called the WUS box, located downstream of the homeodomain in the highly divergent C-terminal region. We found this motif to be well conserved in all proteins of the WUS/WOX1-7 group analyzed (Figure 4), suggesting that this motif is required for the general functioning of WUS/WOX1-7–like proteins. Moreover, we found that all subfamilies terminate with subfamily specific C-terminal motifs that are surprisingly well conserved between dicots and monocots in contrast with what was previously reported (Deveaux et al., 2008). Although these short peptide motifs usually differ between different subfamilies, indicating functional divergence, they are in some cases (partially) shared between different subfamilies (Figure 4), possibly reflecting a putative common origin or function. For example, the C-terminal motif of all WUS orthologs contains an EAR-like motif (LELxL), which is proposed to function as a transcriptional repressor (Kieffer et al., 2006). Interestingly, WOX5 members terminate with a very similar motif, in line with the recently demonstrated homologous function of WOX5 compared with WUS (Sarkar et al., 2007). By contrast, the tree topology in itself does not provide any clue of a functional relationship between WOX5 and WUS subfamilies. Likewise, the structural and peptide motif analysis reveal a closer sequence relationship between WOX1 and WOX4 members than to other subfamilies, which could not have been concluded based on the topology of the WOX tree alone: WOX1 and WOX4 proteins within the WUS/WOX1-7 group uniquely share an exon upstream of the homeodomain, and in this exon a small peptide motif (named 5′ WOX1/4 motif) is found that is well conserved between WOX1 and WOX4 members (Figure 4). Such a combined phylogenetic and structural analysis therefore might be helpful to provide a framework for future studies involving other members of the WOX family.

Here, we used this approach to determine a putative *Arabidopsis MAW* ortholog: All investigated criteria (position in the tree, conservation of exon/intron structure, and occurrence of small conserved peptide motifs) independently determine *WOX1* as the putative *MAW* ortholog in *Arabidopsis*, while *PFS2*/*WOX6* together with poplar *WOX6* encode more divergent members of the *WOX1* subfamily (Figure 4). Due to divergence in their homeodomain, phylogenetic positioning of these *WOX6* genes to the *WOX1* subfamily is not well supported in our study and has remained unresolved in earlier published *WOX* phylogenies (Haecker et al., 2004; Nardmann and Werr, 2006; Nardmann et al., 2007; Deveaux et al., 2008). Nevertheless, conservation of genomic structure (four exons) and the presence of a *WOX1*-specific C-terminal motif make it highly improbable that *WOX6*/*PFS2* and poplar *WOX6* would classify to a different subfamily.

WOX1 and *PRS* Redundantly Encode a Function Similar to *MAW* in Petunia

To compare *WOX1* function with *MAW*, we analyzed *wox1* knockout alleles, but surprisingly, no obvious phenotype could be observed. This demonstrates that in contrast with its ortholog in petunia, loss of *WOX1* function can be fully compensated for by other factors under the applied growth conditions. Subsequently, we tested for a possible genetic redundancy between *WOX1* and *WOX6*/*PFS2* (Park et al., 2004, 2005), since *WOX6*/*PFS2* represents another (though divergent) member of the *Arabidopsis WOX1* clade (Figure 4). However, *wox1 wox6* mutants also did not display a *maw*-like phenotype, showing that a putative redundancy between the two *WOX1* clade members in *Arabidopsis* is not sufficient to explain the wild-type appearance of *wox1* mutants compared with *maw* in petunia. This is in accordance with the divergent characteristics of *WOX6*/*PFS2* compared with the other members of the *WOX1* subfamily.

The observed leaf blade reduction in both petunia *maw* (*WOX1* subfamily) and maize *ns* mutants (*PRS* subfamily) together with the absence of a clear leaf blade phenotype in *Arabidopsis wox1 wox6* and *prs* mutants suggested a possible overlap in function between *WOX1* and *PRS* subfamily members in *Arabidopsis*. The phenotype of *wox1 prs* mutants indeed confirms this hypothesis, showing that *WOX1* and *PRS* redundantly encode a function similar to *MAW* and that the broader function of *PRS* in leaf and flower development has so far been obscured by redundancy with *WOX1*.

Interestingly, this finding also offers a logical explanation for the absence of a leaf blade phenotype in *prs* compared with maize *ns1 ns2* mutants (Nardmann et al., 2004): Combined with the observation that the *WOX1* subfamily seems to be lacking in grasses such as maize, rice, *Brachypodium* (Nardmann and Werr, 2006; Nardmann et al., 2007), and sorghum (Figure 4), this indicates that the differences in phenotype can be attributed to the activity of the *MAW*/*WOX1* subfamily in *Arabidopsis*. Remarkably, poplar does contain two clear *WOX1* orthologous sequences but seems to lack a *WOX3*/*PRS*-like gene (Figure 4; Nardmann and Werr, 2006; Nardmann et al., 2007). This further indicates that the *WOX* gene family has been subject to intensive diversification during evolution (see also last paragraph).

A Putative Role for *WOX* Genes in Dorsoventral Patterning?

Petunia *maw*, *chsu*, and *maw chsu* mutants and *Arabidopsis wox1 prs* mutants display a reduction of lateral outgrowth of the leaf blade and floral organs, a phenotype previously reported for the maize *ns1 ns2* mutant (Scanlon et al., 2000; Nardmann et al., 2004). Based on fate mapping and the phenotype of *ns1 ns2* mutants (Scanlon et al., 2000), the *NS* genes have been proposed to be involved in the recruitment of leaf founder cells from a lateral compartment of maize meristems, as such explaining the deletion of a lateral region of the leaf blade (Nardmann et al., 2004).

In addition to the observed blade reduction in the petunia and *Arabidopsis* mutants analyzed here, we also observed morphological changes that suggest polarity defects along the abaxial/adaxial axis. These defects occur mainly at the organ margins of *maw* and *wox1 prs* mutants but are dramatically enhanced in *maw chsu* double mutants, which frequently develop nearly fully radialized leaves and floral organs.

Leaf development has been studied extensively in *Arabidopsis*, and it has been demonstrated that lateral outgrowth of the leaf blade (and floral organs) depends on an equilibrated interaction between adaxial and abaxial growth promoting factors. With some exceptions, these polarity determinants exhibit a polarized expression pattern along the dorsoventral axis. These include, among others, members of the homeodomain leucine zipper III (*HD-ZIPIII*) family, which are expressed adaxially where they promote adaxial fate (McConnell and Barton, 1998; McConnell et al., 2001; Emery et al., 2003; Prigge et al., 2005), while *KAN* genes (Kerstetter et al., 2001; Emery et al., 2003; Wu et al., 2008), *YAB* genes (Sawa et al., 1999; Siegfried et al., 1999; Eshed et al., 2004), and specific members of the *ARF* (Pekker et al., 2005) gene family are expressed abaxially, where they specify abaxial fate. In addition, *ARF4* and *ETT* are also expressed in the provascular tissue (Pekker et al., 2005) during leaf development (see below).

Expression of *PRS* and *NS* genes is restricted to the margins in developing leaves and floral organs. *MAW* and *WOX1* are expressed in a stripe across organ primordia and overlap with *PRS* in the marginal regions in *Arabidopsis* (the expression pattern of petunia *WOX3*/*PRS* remains to be determined). Given this spatial expression pattern, it is unlikely that *PRS* and *MAW*/*WOX1* genes act as primary abaxial/adaxial identity determinants. Nevertheless, the observed marginal abaxialization events indicate that these genes interfere with the balance between adaxial and abaxial domains, which normally converge at the margin of developing organs. This suggests that an abaxial/adaxial disequilibrium at the margin might also contribute to the observed reduction in lamina outgrowth. We have investigated this by monitoring the expression level of a number of dorsoventral determinants in wild-type and mutant backgrounds. In the petunia single *maw* and *chsu* mutants and in *Arabidopsis wox1 prs* double mutants, only a subtle upregulation of the abaxial determinants *ARF4* and *ETT* is observed. By contrast, this upregulation is well pronounced in *maw chsu* double mutants, while enhanced *KAN* expression also becomes apparent. This fully correlates with the severity of the respective phenotypes of *maw chsu* mutants compared with the petunia single mutants and *Arabidopsis wox1 prs* mutants. It further indicates that the leaf phenotype of *maw* and *prs wox1* mutants might be too subtle to analyze all the molecular downstream effects of these mutations in a straightforward fashion. The *maw chsu* mutant clearly is better suited for such an approach, but unfortunately, the regulatory network for dorsoventral patterning remains to be characterized in petunia. The identification of additional factors acting redundantly with *WOX1* and *PRS* in *Arabidopsis* leaf development to obtain a stronger mutant phenotype might be a more straightforward approach to facilitate such a downstream analysis. Nevertheless, the analysis of *maw chsu* mutants has provided a first clue how *WOX* genes might be involved in the regulation of dorsoventral patterning. Upregulation of the abaxial determinants *ARF4*, *ETT*, and *KAN* is consistent with the strongly abaxialized *maw chsu* organs and suggests that *WOX* genes might repress the activities of these genes. As the expression of *WOX1* in the provascular tissues of developing leaves and of *PRS* in the leaf margins resides completely within the *ETT* and *ARF4* expression domains (Pekker et al., 2005), this implies that such a putative repression function of *ARF4* and *ETT* (directly or indirectly) should act in a quantitative matter.

Finally, comparison of pathways regulating leaf development has revealed a surprising divergence between dicots and monocots in several aspects (Kidner and Timmermans, 2007). Thus, the extent of the similarity between the functions of *NS*, on one hand, and *PRS* together with *WOX1*, on the other hand, remains to be investigated.

Functional Divergence in the WOX Gene Family

While developmental defects in leaves, bracts, sepals, and petals are comparable between *maw* and *wox1 prs* mutants, there is a striking difference in pistil phenotypes. In petunia, loss of *MAW* function has a direct effect on reproductive success because carpel fusion defects in the pistil strongly reduce female fertility. By contrast, pistil development and fertility seem unaffected in *wox1 prs* double mutants, despite the pronounced phenotype observed in the other floral organs and leaves. The complete absence of a phenotype in *wox1* single mutants, together with the absence of a pistil phenotype in *wox1 prs* double mutants, demonstrate that *MAW* has evolved toward a more unique role compared with its ortholog *WOX1*. To establish fully the molecular mechanism of this diversification will require the additional comparative analysis of other *WOX* genes potentially involved in this process and swapping experiments between petunia and *Arabidopsis*. This should also elucidate to what extent the complete set of target genes regulated by either *MAW* or *PRS*/*WOX1* have been conserved.

In addition, it is clear that the putative petunia *WOX3*/*PRS* homolog (which remains to be characterized; Figure 4), cannot rescue wild-type leaf development in a *maw* genetic background, in the way that *PRS* does in *Arabidopsis wox1* mutants. The latter observation in *Arabidopsis* is quite remarkable because synergistic phenotypes, such as those seen in *prs wox1* mutants, normally occur between mutants of closely related genes, whereas members of the *WOX1* and *PRS* subfamilies are structurally quite divergent (Figure 4). This study indicates that despite their sequence divergence, a basal function in lateral

organ development has been redundantly maintained in both subfamilies. This begs the question whether other members of the *WUS*/*WOX1-7* clade perhaps share (other) redundant functions with either *WOX1* and/or *PRS* clade members. Recently, it was shown that *PRS* and *WOX1* act redundantly with *WOX2* and *WOX5* in patterning of the shoot during embryo development (Breuninger et al., 2008).

Together, our results indicate a conserved role for *MAW*/*WOX1*/*PRS* genes in regulating lateral organ development; they also suggest differential recruitment of *WOX* gene function depending on species and organ type. Our comparative data together with previous reports on *WOX* gene function and phylogeny in different species identify the *WOX* gene family as highly dynamic and, therefore, an attractive subject for future evo-devo studies.

METHODS

Plant Material and Growth Conditions

Petunia (*Petunia* × *hybrida*) lines were grown in soil in a greenhouse. All petunia mutants described in this work arose spontaneously among progeny of the W138 line (Gerats et al., 1990). We identified the recessive *maw-1*, *maw-4*, *maw-5*, and *chsu* mutants in a forward screening for petal fusion defects and the *maw-2* and *maw-3* mutants by screening three-dimensionally pooled W138 insertion libraries (Koes et al., 1995; Vandenbussche et al., 2003b) for new independent insertions in *MAW*. dTph1 transposon insert positions for *maw-1* to *-5* alleles were determined by sequencing and are indicated in Figure 3A.

All *Arabidopsis thaliana* mutants were in the Columbia background, and plants were grown on soil under a long photoperiod (16 h light/8 h dark) at 22°C in a growth chamber. The T-DNA insertion mutants *wox6* (SALK_033323) and *prs* (SALK_127850) were obtained from the SALK collection (Alonso et al., 2003). The SALK_033323 line corresponds to the earlier described *pfs2-2* allele (Park et al., 2005). *wox1 En1* transposon insertion lines (lines 7AAF56, 8AAJ85, 7AAH104, and J37/41) were obtained from the ZIGIA transposon collection of the Max Planck Institute for Plant Breeding Research (Steiner-Lange et al., 2001). A graphic representation of all *Arabidopsis* insertion lines used in this study is shown in Supplemental Figure 5 online, indicating exact insert positions as determined by sequencing of these lines.

Cloning of *MAW* by Transposon Display and Genotyping of *maw* and *chsu* Mutants

By transposon display (Van den Broeck et al., 1998), we identified a single 220-bp *dTph1* transposon-flanking fragment present in 10 homozygous and 11 heterozygous *maw-1* mutants and absent in 15 homozygous wild-type plants (see Supplemental Figure 1 online). This fragment was cloned in pGEM-T (Promega) for sequencing and was further extended to obtain full-length genomic and cDNA clones by rapid amplification of cDNA ends (RACE)-PCR (Clontech) and Genome Walking (Clontech).

To identify new *maw* insertion alleles, we screened three-dimensionally pooled insertion libraries with a *MAW*-specific primer m227 in combination with the IR88 primer complementary to the terminal inverted repeat of the *dTph1* transposon (see Supplemental Table 1 online). Segregation analysis of the five independent *maw* alleles (*maw-1* to *-5*) was done by PCR using gene-specific primer pairs flanking the insertion sites (see Supplemental Table 1 online). For *maw chsu* double mutant analysis, we crossed *maw-3* and *maw-4* alleles with *chsu* mutants, yielding identical phenotypes for *maw-3 chsu* and *maw-4 chsu* double mutants in the F2 generation. Genotyping of F2 individuals derived from these crosses was done by PCR for *maw* alleles and by backcrossing with homozygous *chsu* mutants.

Characterization of *Arabidopsis WOX1*, *WOX6*/*PFS2*, and *PRS*/*WOX3* Insertion Alleles and Genotyping

All primers used for the following work are listed in Supplemental Table 1 online. The effect of the various *En1* transposon and T-DNA *WOX* gene insertions on transcription levels was monitored by RT-PCR (see Supplemental Figure 5 online) using gene-specific primers flanking the insertion sites. RNA for this analysis was isolated from young developing flowers, and equal RNA amounts were used for cDNA synthesis as described earlier (Vandenbussche et al., 2004). Expression of *ACTIN* (*ACT2*) was used as a positive control for cDNA synthesis (25 cycles). Results of reactions (35 cycles) for *wox1*, *wox6*, and *prs* expression are shown in Supplemental Figure 5 online. Genotyping of the *wox6* and *prs* lines was done by PCR using insertion flanking gene-specific primer pairs in combination with the T-DNA Lba1 primer. Of the four *wox1* insertion alleles (see Supplemental Figure 5A online), only the two exon insertion lines (l7AAF56 and 8AAJ85) were used for further crosses. Genotyping of these lines was done by PCR using insertion flanking gene-specific primer pairs in combination with an *En1* transposon primer.

Electron Microscopy

Samples for cryoscanning electron microscopy were first frozen in slush, prepared in an Oxford Alto 2500 cryo-system (Catan), and then analyzed in a JEOL JSM-6330F field emission electron scanning microscope. Leaf cross sections were obtained by fracturing the leaf blade after freezing. False colors were added using Paint Shop Pro 6 (Jasc Software).

Quantitative Real-Time RT-PCR Analysis

Relative expression levels in various tissues were determined by quantitative real-time RT-PCR analysis (see Supplemental Figure 2 online and Figure 6) in a MyiQ single-color real-time PCR machine (Bio-Rad) as described earlier (Rijpkema et al., 2006) and normalized against *ACTIN* expression levels using MyiQ software (Bio-Rad) with default settings. Primers used for the expression analysis were designed using Beacon Designer (www.PremierBiosoft.com) and are shown in Supplemental Table 1 online. Differential expression values between mutant and wild-type samples were tested for statistical significance by a one-way analysis of variance test in SPSS 15.0 for windows, using Tukey HSD as post hoc test.

In Situ Hybridization

For in situ hybridization, *MAW* and *WOX1* probes were chosen derived from the region downstream of the conserved homeodomain to prevent cross-hybridization to other homeobox genes. The probe templates were generated by PCR using gene-specific primers (see Supplemental Table 1 online) and subsequently cloned in pGEM-T (Promega), containing T7 and SP6 transcription sites. Probe synthesis and in situ hybridizations were performed as described previously (Cañas et al., 1994; Vandenbussche et al., 2004). Images were recorded with an AxioCam digital camera (Zeiss).

Subcellular Localization of Petunia eGFP-MAW Fusion Proteins

The full coding sequence of *MAW* was amplified using gene-specific primers containing partial Gateway recombination sites (see Supplemental Table 1 online) and cloned in pdonR221 (Invitrogen) and introduced into p7WGF2 (Karimi et al., 2002) This plasmid was transformed into *Agrobacterium tumefaciens* strain LBA4404.pBBR1MC-5-virGN54D (van

der Fits et al., 2000) for the transfection of tobacco (*Nicotiana tabacum*) BY-2 cells as described earlier (Geelen and Inze, 2001). Images were made with a confocal laser scanning microscope (LSM510; Carl Zeiss), using a ×63 water immersion objective (numerical aperture of 1.2). The excitation light was provided by the 488-nm light of an argon laser set at full power (8.1 A; 15 mW). A 488-nm dichroic beam splitter was reflecting the excitation light, while the emission light was transmitted and passed through a 505- to 530-nm band-pass filter. Zeiss LSM510 software (version 2.01) was used to analyze the images.

Cloning of Additional Petunia WOX Family Members *WOX2*, *WOX3*, and *WOX4*

WOX2 and *WOX4* were amplified from cDNA derived from young floral buds using the degenerate primer M544 in a 3′ RACE-PCR (Ambion). A fragment of *WOX3* was amplified using the degenerate primer pair m974 and m469. Full-length sequences were obtained by 5′ and 3′ RACE-PCR (Ambion). Sequences of the primers used for cloning are in Supplemental Table 1 online.

Phylogenetic Analysis and Structural Annotation of the *WOX* Gene Family

In a first step, we extracted all available putative WOX proteins from the fully sequenced genomes of three eudicot species (*Arabidopsis*, *Populus trichocarpa*, and *Vitis vinifera*) and of two monocot species (*Oryza sativa* and *Sorghum bicolor*) using the National Center for Biotechnology Information (http://www.ncbi.nlm.nih.gov/), Joint Genome Initiatve (http://genome.jgi-psf.org/), GRAMENE (http://www.gramene.org/), and the Orygene (http://orygenesdb.cirad.fr) databases. The automatic prediction of the corresponding gene models and putative proteins was individually checked and compared between orthologous sequences from the different species. In a limited number of cases, erroneous annotation was suspected based on strongly aberrant gene structures or peptide sequences. We reannotated these sequences using Genemark.hmm (Lomsadze et al., 2005), which resulted in all cases in newly predicted putative proteins fitting much closer the expected structural conservation between orthologs. Reannotated sequences that deviate from predictions in the databases have been marked by an asterisk in Figure 3, and annotation remarks have been added in Supplemental Table 2 online. A comparison between old and newly predicted protein sequences can be found in Fasta format as Supplemental Data Set 1 online. Next, all sequences representing the petunia WOX proteins isolated in this study were added, together with a selection of functionally characterized WOX proteins from other species (see Supplemental Table 2 online). We named the grapevine sequences and the additional petunia proteins according to their homology with members of the *Arabidopsis* WOX family. For poplar, 12 of the 18 identified WOX proteins corresponded to partial sequences described earlier (Nardmann and Werr, 2006; Nardmann et al., 2007), for which we have maintained their original nomenclature. The remaining poplar sequences were named based on their phylogenetic position. All protein sequences were subsequently aligned using ClustalW (Thompson et al., 1994) using default settings. This alignment was checked manually and edited using BioEdit (Hall, 1999) to refine the alignment of the short conserved peptide motifs upstream and downstream of the conserved homeodomain (see Supplemental Data Set 1 online). For the phylogenetic analysis, only the homeodomain region was used, and it was aligned independently (see Supplemental Figure 3 and Supplemental Data Set 2 online). The neighbor-joining tree based on this homeodomain region was computed with Treecon software (Van de Peer and De Wachter, 1994) using default settings. To assess the support for the inferred relationships, 1000 bootstrap samples were generated. Structural organization of the WOX1-7 clade members included in the tree was determined by comparing predicted coding sequences with genomic sequences when available.

Accession Numbers

Sequence data described in this article can be found in the GenBank data libraries under the following accession numbers: Ph-*MAW*, EU359004; Ph-*WOX2*, EU359005; Ph-*WOX3*, FJ628172; Ph-*WOX4*, EU359006; Ph-*YAB1*, EU359007; Ph-*KAN1*, GQ475532; Ph-*ARF4*, GQ475533; and Ph-*ETT*, GQ475531. Genome Initiative locus identifiers and accession codes for the genes mentioned in this article are shown in Supplemental Tables 1 and 2 online. Seeds from homozygous *wox1* and *wox1 prs* mutants have been deposited at the Nottingham Arabidopsis Stock Centre (NASC).

Supplemental Data

The following materials are available in the online version of this article.

Supplemental Figure 1. Cloning of the MAW Locus by Transposon Display.

Supplemental Figure 2. MAW Expression Analysis by qRT-PCR.

Supplemental Figure 3. Alignment of the Homeodomain Region Used for the Construction of the NJ Tree.

Supplemental Figure 4. Full NJ Tree of the WOX Homeodomain Family.

Supplemental Figure 5. Characterization of *Arabidopsis* WOX Insertion Lines Used in This Study.

Supplemental Figure 6. Overview of all *Arabidopsis* Phenotypes Obtained in This Study.

Supplemental Table 1. Oligo Sequences Used in This Study.

Supplemental Table 2. Accession Code Table of the Sequences Used in the Phylogenetic Analysis

Supplemental Data Set 1. Full Protein Sequences of All WOX Family Members Described in the Tree.

Supplemental Data Set 2. Alignment of the Homeodomain Region Used for the Construction of the NJ Tree.

ACKNOWLEDGMENTS

We thank the Salk Institute Genomic Analysis Laboratory for providing the sequence-indexed *Arabidopsis* T-DNA insertion mutants and the ABRC and NASC for providing these lines, the ZIGIA Consortium for screening of *wox1* transposon insertion alleles and for providing seeds of these lines, Jeroen Stuurman for the gift of the *chsu* mutant, and Geert-Jan Janssen and Mieke Wolters for technical assistance. M.V. thanks S. Rodrigues Bento for inspiration and support. We also thank the anonymous reviewers for useful suggestions and comments. The work of A.R. is funded by the Netherlands Organization for Scientific Research (Grant 814.02.009).

Received January 23, 2009; revised July 20, 2009; accepted August 7, 2009; published August 28, 2009.

REFERENCES

Alonso, J.M., et al. (2003). Genome-wide insertional mutagenesis of *Arabidopsis thaliana*. Science **301:** 653–657.

Ando, T., Nomura, M., Tsukahara, J., Watanabe, H., Kokubun, H.,

Tsukamoto, T., Hashimoto, G., Marchesi, E., and Kitching, I.J. (2001). Reproductive isolation in a native population of *Petunia sensu* Jussieu (Solanaceae). Ann. Bot. (Lond.) **88:** 403–413.

Breuninger, H., Rikirsch, E., Hermann, M., Ueda, M., and Laux, T. (2008). Differential expression of WOX genes mediates apical-basal axis formation in the Arabidopsis embryo. Dev. Cell **14:** 867–876.

Cañas, L.A., Busscher, M., Angenent, G.C., Beltran, J.P., and Van Tunen, A.J. (1994). Nuclear localization of the petunia MADS box protein FBP1. Plant J. **6:** 597–604.

Deveaux, Y., Toffano-Nioche, C., Claisse, G., Thareau, V., Morin, H., Laufs, P., Moreau, H., Kreis, M., and Lecharny, A. (2008). Genes of the most conserved WOX clade in plants affect root and flower development in Arabidopsis. BMC Evol. Biol. **8:** 291.

Emery, J.F., Floyd, S.K., Alvarez, J., Eshed, Y., Hawker, N.P., Izhaki, A., Baum, S.F., and Bowman, J.L. (2003). Radial patterning of Arabidopsis shoots by class III HD-ZIP and KANADI genes. Curr. Biol. **13:** 1768–1774.

Eshed, Y., Izhaki, A., Baum, S.F., Floyd, S.K., and Bowman, J.L. (2004). Asymmetric leaf development and blade expansion in Arabidopsis are mediated by KANADI and YABBY activities. Development **131:** 2997–3006.

Garcia, D., Collier, S.A., Byrne, M.E., and Martienssen, R.A. (2006). Specification of leaf polarity in Arabidopsis via the trans-acting siRNA pathway. Curr. Biol. **16:** 933–938.

Geelen, D.N., and Inze, D.G. (2001). A bright future for the bright yellow-2 cell culture. Plant Physiol. **127:** 1375–1379.

Gerats, A.G., Huits, H., Vrijlandt, E., Marana, C., Souer, E., and Beld, M. (1990). Molecular characterization of a nonautonomous transposable element (dTph1) of petunia. Plant Cell **2:** 1121–1128.

Haecker, A., Gross-Hardt, R., Geiges, B., Sarkar, A., Breuninger, H., Herrmann, M., and Laux, T. (2004). Expression dynamics of WOX genes mark cell fate decisions during early embryonic patterning in *Arabidopsis thaliana*. Development **131:** 657–668.

Hall, T.A. (1999). BioEdit: A user-friendly biological sequence alignment editor and analysis program for Windows 95/98/NT. Nucleic Acids Symp. Ser. **41:** 95–98.

Hoballah, M.E., Gubitz, T., Stuurman, J., Broger, L., Barone, M., Mandel, T., Dell'Olivo, A., Arnold, M., and Kuhlemeier, C. (2007). Single gene-mediated shift in pollinator attraction in petunia. Plant Cell **19:** 779–790.

International Rice Genome Sequencing Project (2005). The map-based sequence of the rice genome. Nature **436:** 793–800.

Iwakawa, H., Ueno, Y., Semiarti, E., Onouchi, H., Kojima, S., Tsukaya, H., Hasebe, M., Soma, T., Ikezaki, M., Machida, C., and Machida, Y. (2002). The ASYMMETRIC LEAVES2 gene of *Arabidopsis thaliana*, required for formation of a symmetric flat leaf lamina, encodes a member of a novel family of proteins characterized by cysteine repeats and a leucine zipper. Plant Cell Physiol. **43:** 467–478.

Jaillon, O., et al. (2007). The grapevine genome sequence suggests ancestral hexaploidization in major angiosperm phyla. Nature **449:** 463–467.

Jiang, C., Gu, X., and Peterson, T. (2004). Identification of conserved gene structures and carboxy-terminal motifs in the Myb gene family of Arabidopsis and *Oryza sativa* L. ssp. indica. Genome Biol. **5:** R46.

Karimi, M., Inze, D., and Depicker, A. (2002). GATEWAY vectors for Agrobacterium-mediated plant transformation. Trends Plant Sci. **7:** 193–195.

Kerstetter, R.A., Bollman, K., Taylor, R.A., Bomblies, K., and Poethig, R.S. (2001). KANADI regulates organ polarity in Arabidopsis. Nature **411:** 706–709.

Kidner, C.A., and Timmermans, M.C. (2007). Mixing and matching pathways in leaf polarity. Curr. Opin. Plant Biol. **10:** 13–20.

Kieffer, M., Stern, Y., Cook, H., Clerici, E., Maulbetsch, C., Laux, T., and Davies, B. (2006). Analysis of the transcription factor WUSCHEL and its functional homologue in Antirrhinum reveals a potential mechanism for their roles in meristem maintenance. Plant Cell **18:** 560–573.

Koes, R., et al. (1995). Targeted gene inactivation in petunia by PCR-based selection of transposon insertion mutants. Proc. Natl. Acad. Sci. USA **92:** 8149–8153.

Laux, T., Mayer, K.F., Berger, J., and Jurgens, G. (1996). The WUSCHEL gene is required for shoot and floral meristem integrity in Arabidopsis. Development **122:** 87–96.

Li, H., Xu, L., Wang, H., Yuan, Z., Cao, X., Yang, Z., Zhang, D., Xu, Y., and Huang, H. (2005). The putative RNA-dependent RNA polymerase RDR6 acts synergistically with ASYMMETRIC LEAVES1 and 2 to repress BREVIPEDICELLUS and microRNA165/166 in *Arabidopsis* leaf development. Plant Cell **17:** 2157–2171.

Lin, W.C., Shuai, B., and Springer, P.S. (2003). The *Arabidopsis* LATERAL ORGAN BOUNDARIES-domain gene ASYMMETRIC LEAVES2 functions in the repression of KNOX gene expression and in adaxial-abaxial patterning. Plant Cell **15:** 2241–2252.

Lomsadze, A., Ter-Hovhannisyan, V., Chernoff, Y.O., and Borodovsky, M. (2005). Gene identification in novel eukaryotic genomes by self-training algorithm. Nucleic Acids Res. **33:** 6494–6506.

Matsumoto, N., and Okada, K. (2001). A homeobox gene, PRESSED FLOWER, regulates lateral axis-dependent development of Arabidopsis flowers. Genes Dev. **15:** 3355–3364.

Mayer, K.F., Schoof, H., Haecker, A., Lenhard, M., Jurgens, G., and Laux, T. (1998). Role of WUSCHEL in regulating stem cell fate in the Arabidopsis shoot meristem. Cell **95:** 805–815.

McConnell, J.R., and Barton, M.K. (1998). Leaf polarity and meristem formation in Arabidopsis. Development **125:** 2935–2942.

McConnell, J.R., Emery, J., Eshed, Y., Bao, N., Bowman, J., and Barton, M.K. (2001). Role of PHABULOSA and PHAVOLUTA in determining radial patterning in shoots. Nature **411:** 709–713.

Nardmann, J., Ji, J., Werr, W., and Scanlon, M.J. (2004). The maize duplicate genes narrow sheath1 and narrow sheath2 encode a conserved homeobox gene function in a lateral domain of shoot apical meristems. Development **131:** 2827–2839.

Nardmann, J., and Werr, W. (2006). The shoot stem cell niche in angiosperms: expression patterns of WUS orthologues in rice and maize imply major modifications in the course of mono- and dicot evolution. Mol. Biol. Evol. **23:** 2492–2504.

Nardmann, J., Zimmermann, R., Durantini, D., Kranz, E., and Werr, W. (2007). WOX gene phylogeny in Poaceae: A comparative approach addressing leaf and embryo development. Mol. Biol. Evol. **24:** 2474–2484.

Park, S.O., Hwang, S., and Hauser, B.A. (2004). The phenotype of Arabidopsis ovule mutants mimics the morphology of primitive seed plants. Proc. Biol. Sci. **271:** 311–316.

Park, S.O., Zheng, Z., Oppenheimer, D.G., and Hauser, B.A. (2005). The PRETTY FEW SEEDS2 gene encodes an Arabidopsis homeodomain protein that regulates ovule development. Development **132:** 841–849.

Paterson, A.H., et al. (2009). The *Sorghum bicolor* genome and the diversification of grasses. Nature **457:** 551–556.

Pekker, I., Alvarez, J.P., and Eshed, Y. (2005). Auxin response factors mediate *Arabidopsis* organ asymmetry via modulation of KANADI activity. Plant Cell **17:** 2899–2910.

Pinon, V., Etchells, J.P., Rossignol, P., Collier, S.A., Arroyo, J.M., Martienssen, R.A., and Byrne, M.E. (2008). Three PIGGYBACK genes that specifically influence leaf patterning encode ribosomal proteins. Development **135:** 1315–1324.

Prigge, M.J., Otsuga, D., Alonso, J.M., Ecker, J.R., Drews, G.N., and Clark, S.E. (2005). Class III homeodomain-leucine zipper gene family

members have overlapping, antagonistic, and distinct roles in *Arabidopsis* development. Plant Cell **17:** 61–76.

Rebocho, A.B., Bliek, M., Kusters, E., Castel, R., Procissi, A., Roobeek, I., Souer, E., and Koes, R. (2008). Role of EVERGREEN in the development of the cymose petunia inflorescence. Dev. Cell **15:** 437–447.

Rijpkema, A.S., Royaert, S., Zethof, J., van der Weerden, G., Gerats, T., and Vandenbussche, M. (2006). Analysis of the petunia TM6 MADS box gene reveals functional divergence within the DEF/AP3 lineage. Plant Cell **18:** 1819–1832.

Sarkar, A.K., Luijten, M., Miyashima, S., Lenhard, M., Hashimoto, T., Nakajima, K., Scheres, B., Heidstra, R., and Laux, T. (2007). Conserved factors regulate signalling in *Arabidopsis thaliana* shoot and root stem cell organizers. Nature **446:** 811–814.

Sawa, S., Watanabe, K., Goto, K., Liu, Y.G., Shibata, D., Kanaya, E., Morita, E.H., and Okada, K. (1999). FILAMENTOUS FLOWER, a meristem and organ identity gene of Arabidopsis, encodes a protein with a zinc finger and HMG-related domains. Genes Dev. **13:** 1079–1088.

Scanlon, M.J., Chen, K.D., and McKnight, C.I. (2000). The narrow sheath duplicate genes: sectors of dual aneuploidy reveal ancestrally conserved gene functions during maize leaf development. Genetics **155:** 1379–1389.

Siegfried, K.R., Eshed, Y., Baum, S.F., Otsuga, D., Drews, G.N., and Bowman, J.L. (1999). Members of the YABBY gene family specify abaxial cell fate in Arabidopsis. Development **126:** 4117–4128.

Steiner-Lange, S., Gremse, M., Kuckenberg, M., Nissing, E., Schächtele, D., Spenrath, N., Wolff, M., Saedler, H., and Dekker, K. (2001). Efficient identification of Arabidopsis knock-out mutants using DNA-arrays of transposon flanking sequences. Plant Biol. **3:** 391–397.

Stuurman, J., Hoballah, M.E., Broger, L., Moore, J., Basten, C., and Kuhlemeier, C. (2004). Dissection of floral pollination syndromes in petunia. Genetics **168:** 1585–1599.

Stuurman, J., Jaggi, F., and Kuhlemeier, C. (2002). Shoot meristem maintenance is controlled by a GRAS-gene mediated signal from differentiating cells. Genes Dev. **16:** 2213–2218.

Thompson, J.D., Higgins, D.G., and Gibson, T.J. (1994). CLUSTAL W: Improving the sensitivity of progressive multiple sequence alignment through sequence weighting, position-specific gap penalties and weight matrix choice. Nucleic Acids Res. **22:** 4673–4680.

Van den Broeck, D., Maes, T., Sauer, M., Zethof, J., De Keukeleire, P., D'Hauw, M., Van Montagu, M., and Gerats, T. (1998). Transposon Display identifies individual transposable elements in high copy number lines. Plant J. **13:** 121–129.

Vandenbussche, M., Janssen, A., Zethof, J., van Orsouw, N., Peters, J., van Eijk, M.J., Rijpkema, A.S., Schneiders, H., Santhanam, P., de Been, M., van Tunen, A., and Gerats, T. (2008). Generation of a 3D indexed Petunia insertion database for reverse genetics. Plant J. **54:** 1105–1114.

Vandenbussche, M., Theissen, G., Van de Peer, Y., and Gerats, T. (2003a). Structural diversification and neo-functionalization during floral MADS-box gene evolution by C-terminal frameshift mutations. Nucleic Acids Res. **31:** 4401–4409.

Vandenbussche, M., Zethof, J., Royaert, S., Weterings, K., and Gerats, T. (2004). The duplicated B-class heterodimer model: Whorl-specific effects and complex genetic interactions in *Petunia hybrida* flower development. Plant Cell **16:** 741–754.

Vandenbussche, M., Zethof, J., Souer, E., Koes, R., Tornielli, G.B., Pezzotti, M., Ferrario, S., Angenent, G.C., and Gerats, T. (2003b). Toward the analysis of the petunia MADS box gene family by reverse and forward transposon insertion mutagenesis approaches: B, C, and D floral organ identity functions require SEPALLATA-like MADS box genes in petunia. Plant Cell **15:** 2680–2693.

Van de Peer, Y., and De Wachter, R. (1994). TREECON for Windows: S software package for the construction and drawing of evolutionary trees for the Microsoft Windows environment. Comput. Appl. Biosci. **10:** 569–570.

van der Fits, L., Deakin, E.A., Hoge, J.H., and Memelink, J. (2000). The ternary transformation system: Constitutive virG on a compatible plasmid dramatically increases Agrobacterium-mediated plant transformation. Plant Mol. Biol. **43:** 495–502.

Velasco, R., et al. (2007). A high quality draft consensus sequence of the genome of a heterozygous grapevine variety. PLoS One **2:** e1326.

Wijsman, H.J.W. (1983). On the interrelationships of certain species of Petunia. II. Experimental data: Crosses between different taxa. Act. Bot. Neerl. **32:** 97–107.

Wu, G., Lin, W.C., Huang, T., Poethig, R.S., Springer, P.S., and Kerstetter, R.A. (2008). KANADI1 regulates adaxial-abaxial polarity in Arabidopsis by directly repressing the transcription of ASYMMETRIC LEAVES2. Proc. Natl. Acad. Sci. USA **105:** 16392–16397.

Wu, X., Chory, J., and Weigel, D. (2007). Combinations of WOX activities regulate tissue proliferation during Arabidopsis embryonic development. Dev. Biol. **309:** 306–316.

Wu, X., Dabi, T., and Weigel, D. (2005). Requirement of homeobox gene STIMPY/WOX9 for Arabidopsis meristem growth and maintenance. Curr. Biol. **15:** 436–440.

Xu, L., Yang, L., Pi, L., Liu, Q., Ling, Q., Wang, H., Poethig, R.S., and Huang, H. (2006). Genetic interaction between the AS1-AS2 and RDR6-SGS3-AGO7 pathways for leaf morphogenesis. Plant Cell Physiol. **47:** 853–863.

Yao, Y., Ling, Q., Wang, H., and Huang, H. (2008). Ribosomal proteins promote leaf adaxial identity. Development **135:** 1325–1334.

Differential Recruitment of *WOX* Genes for Lateral Development and Organ Fusion in *Petunia* and *Arabidopsis*

Michiel Vandenbussche[a], Anneke Horstman[a], Jan Zethof[a], Ronald Koes[b], Anneke Rijpkema[a] and Tom Gerats[a]

[a]Department of Plant Genetics, IWWR, Radboud University Nijmegen, Toernooiveld 1, 6525 ED, Nijmegen, The Netherlands,
[b]Department of Genetics, Vrije Universiteit Amsterdam, 1081 HV Amsterdam, The Netherlands

Supplemental Data

Supplemental Table S1: Oligo Sequences used in this study.
Supplemental Table S2: Accession code table of the sequences used in the phylogenetic analysis
Supplemental Figure S1: Cloning of the MAW locus by Transposon Display.
Supplemental Figure S2: MAW expression analysis by qRT-PCR.
Supplemental Figure S3:.Alignment of the homeodomain region used for the construction of the NJ-Tree.
Supplemental Figure S4: Full NJ tree of the WOX homeodomain family
Supplemental Figure S5: Characterization of *Arabidopsis* WOX insertion lines used in this study
Supplemental Figure S6: Overview of all *Arabidopsis* phenotypes obtained in this study.
Supplemental Fasta file F1: Full protein sequences of all WOX family members described in the tree (fasta file)

Sup. Table 1: Oligonucleotides used in this study

APPLICATION		FORWARD (5' TO 3')		REVERSE (5' TO 3')	REMARKS
PETUNIA x HYBRIDA					
maw insertion screening	IR88	GAATTCGCTCCGCCCCTG	m227	GTCTTTTTTGGCGTTCCCTAGCCTTGTG	
maw1 segregation analysis	m222	TGCAACAAAGAAGGAGCCTACTAG	m219	TTCCATAGTTCTTGGTGTTGATGGAC	
maw2 segregation analysis	m220	AAAAAGCAGGCTCAACAATGTGGATGATGGGTTACAAT GAC	m254	AAAGTCATCTCCATGAATGCTTC	
maw3 segregation analysis	m229	TAGTGGTGAGTTCACGTTGGAATCC	m227	GTCTTTTTTGGCGTTCCCTAGCCTTGTG	
maw4&5 segregation analysis	m373	TGGCAGAATATAGATCAGCAGA	m219	TTCCATAGTTCTTGGTGTTGATGGAC	
MAW GFP fusion constructs	m220	AAAAAGCAGGCTCAACAATGTGGATGATGGGTTACAAT GAC	m221	AGAAAGCTGGGTAATTCCTAGTCTCTTGATCTTCCT	
MAW in situ probe synthesis	m216	CAGTCCATCAACACCAAGAACTATGGA	m409	GATACATATCATTGAACCACATCATTAC	
MAW Q-PCR analysis	m220	AAAAAGCAGGCTCAACAATGTGGATGATGGGTTACAAT GAC	m227	GTCTTTTTTGGCGTTCCCTAGCCTTGTG	
PhWOX2,PhWOX4 cloning	m544	AAYGTBTTYTAYTGGTTTCARAAYCAYAAAGC			
PhWOX3 cloning	m974	TGGAIYCCNACIMMIGANCAA	m469	GCCTTATGRTTYTGRAACCARTARAAVACATT	
ARABIDOPSIS THALIANA					
Zigia lines segregation analysis	En205	AGAAGCACGACGGCTGTAGAATAGGA	En8130	GAGCGTCGGTCCCCACACTTCTATAC	En transposon
At-wox1-7AAF56 segregation analysis	m263	ATGTGGACGATGGGTTACAACG	m358	AGAAACAAGGGAAAGAGAGACTGGA	in comb. with En8130
At-wox1-8AAJ85 segregation analysis	m359	CACAGCAGTGGTGACGATGACG	m292	CTTCAAGAACCCTTAACTGATCTGGTG	in comb. with En205
At-wox1-8AAJ85 expression analysis	m359	GCAGTGGTGACGATGACG	m292	CTTCAAGAACCCTTAACTGATCTGGTG	
At-wox1 In situ probe synthesis	m293	CAGAAACGACGGCGACAAATGGA	m264	AGAAAGCTGGGTTAGTTCTTCAATGGCAGAAACTCA TAG	
Salk lines segregation analysis	Lba1	TGGTTCACGTAGTGGGCCATCG			T-DNA primer
At-wox6-pfs2SALK_033323 segregation. analysis	m379	TAAAGACGTCAAGGATTCATCATCAG	m380	GAGCTTTGTCTGATCAACTCGATG	in comb. with Lba1
At-wox6/pfs2-SALK_033323 expression analysis	m400	ATGGGCTACATCTCCAACAACAAC	m380	GAGCTTTGTCTGATCAACTCGATG	
At-PRS/WOX3 Salk_127850 segregation analysis	m784	GGGAACTGGAGTAGGAGAAGCTC	m785	CATCCAATCTCGACCGTACGATGAG	in comb. with Lba1
At-PRS/WOX3 Salk_127850 expression analysis	m784	GGGAACTGGAGTAGGAGAAGCTC	m785	CATCCAATCTCGACCGTACGATGAG	
At-actin2 Expression analysis	m909	GAGAGGTTACATGTTCACCACAAC	m910	GTGAACGATTCCTGGACCTGCCTC	

Sup. Table 2: Accession code table of the sequences used in the phylogenetic analysis

Clade ID...	*Arabidopsis thaliana*	*Vitis vinifera*	*Populus trichocarpa*	*Oryza sativa*	*Sorghum bicolor*
WUS	At-WUS AT2G17950	Vv-WUS GSVIVG00036791001	Pt-WUS grail3.0019031001	Os04g56780	Sb06g031880
			Pt-WUSB estExt_fgenesh4_pg.C_570090		
WOX1	AT-WOX1 AT3G18010	Vv-WOX1A CAN59842	Pt-WOX1A* AM234756 (partial)	No ortholog	No ortholog
		Vv-WOX1B* VV78X078650.7	Pt-WOX1B* AM234757 (partial)		
WOX6/ PFS2	AT-WOX6 AT2G01500	No ortholog	Pt-WOX6 fgenesh1_pg.C_LG_X001034	No ortholog	No ortholog
WOX2	AT-WOX2 AT5G59340	Vv-WOX2 CAO21685	Pt-WOX2 fgenesh4_pg.C_LG_I001778	Os01g62310	Sb03g039380
			Pt-WOX2B eugene3.00091351 (JGI))		
WOX3/ PRS	AT-WOX3/PRS AT2G28610	Vv-WOX3 CAN60351	No ortholog	Os05g02730	Sb09g002010
				Os11g01130	Sb05g003490
WOX4	AT-WOX4 AT1G46480	Vv-WOX4 CAN76463	Pt-WOX4 estExt_fgenesh4_pm.C_400124	Os04g55590	Sb06g030700
			Pt-WOX4B estExt_Genewise1_v1.C_LG_II2767		
WOX5/7	At-WOX5 AT3G11260	Vv-WOX5 CAO69022	Pt-WOX5/7-B fgenesh4_pm.C_LG_X000761	Os01g63510	Sb03g040210
	At-WOX7* AT5G05770		Pt-WOX5/7-A*		
WOX8/9	At-WOX8/STPL AT5G45980				
	WOX9/STIP AT2G33880	Vv-WOX9*	Pt-WOX9 eugene3.00040441	Os05g48990	Sb09g028562
			Pt-WOX9B gw1.187.73.1	Os07g34880	
				Os01g47710	
WOX11/12	WOX11 AT3G03660	Vv-WOX11/12 CAO67473	Pt-WOX11/12A eugene3.00130648 & eugene3.00130647 (2 cop.)	Os08g14400	Sb07g007600
	WOX12 AT5G17810		Pt-WOX11/12B fgenesh4_pm.C_LG_XIX000125	Os03g20910	Sb01g036670
				Os07g48560	Sb02g043300
WOX13	At-WOX13 AT4G35550	Vv-WOX13A CAO66249	Pt-WOX13 grail3.0026036101	Os01g60270	Sb03g038080
		Vv-WOX13B CAO14479	Pt-WOX13B grail3.0002080401 (JGI)		
		Vv-WOX13C CAO14480	Pt-WOX13C estExt_fgenesh4_pg.C_LG_II0076		
WOX10/14	At-WOX10 AT1G20710			No ortholog	No ortholog
	At-WOX14 AT1G20700				

Other WOX proteins included in the phylogenetic analysis

Clade id	Species	Gene name	Accession code	reference
WUS	*Petunia x hybrida*	TER (WUS)	AAM90847	(Stuurman et al., 2002)
	Antirrhinum majus	ROA	AAO23113	(Kieffer et al., 2006)
WOX1	*Petunia x hybrida*	MAEWEST (Ph-WOX1)	EU359004	This study
WOX2	*Petunia x hybrida*	Ph-WOX2	EU359005	This study
WOX4	*Petunia x hybrida*	Ph-WOX4	EU359006	This study
WOX3	*Petunia x hybrida*	Ph-WOX3	FJ628172	This study
	Zea mays	NS1	Q70UV1	(Nardmann et al., 2004)
	Zea mays	NS2	AAR31212	(Nardmann et al., 2004)
Sp,WOX8/9	*Petunia x hybrida*	EVG	EF187281	(Rebocho et al., 2008)
WOX8/9	*Petunia x hybrida*	SOE	EF187282	(Rebocho et al., 2008)

(Re)-Annotation remarks: (see also Sup. Fasta file F1 for alternative protein models)

At-WOX7*	Only one exon in database, with genemark.hmm 2 exons predicted, terminating with conserved WUS/WOX5 clade c-terminal motif
Vv-WOX1B*	5exons predicted in CAN77014.1, 4exons predicted with genemark.hmm on Vitis vinifera contig VV78X078650.7
Vv-WOX9*	Genemark.hmm prediction generates longer C-terminal end than in CAO66373, including strongly conserved C-terminal motifs found in WOX8/9//11/12 proteins
Pt-WOX1A*	AM234756 database seq is only partial, full length protein predicted with genemark.hmm
Pt-WOX1B*	AM234757 database seq is only partial, full length protein predicted with genemark.hmm
Pt-WOX5/7-A*	Only one exon predicted in grail3.0049030001, with genemark.hmm 2 exons predicted, terminating with conserved WUS/WOX5 clade c-terminal motif

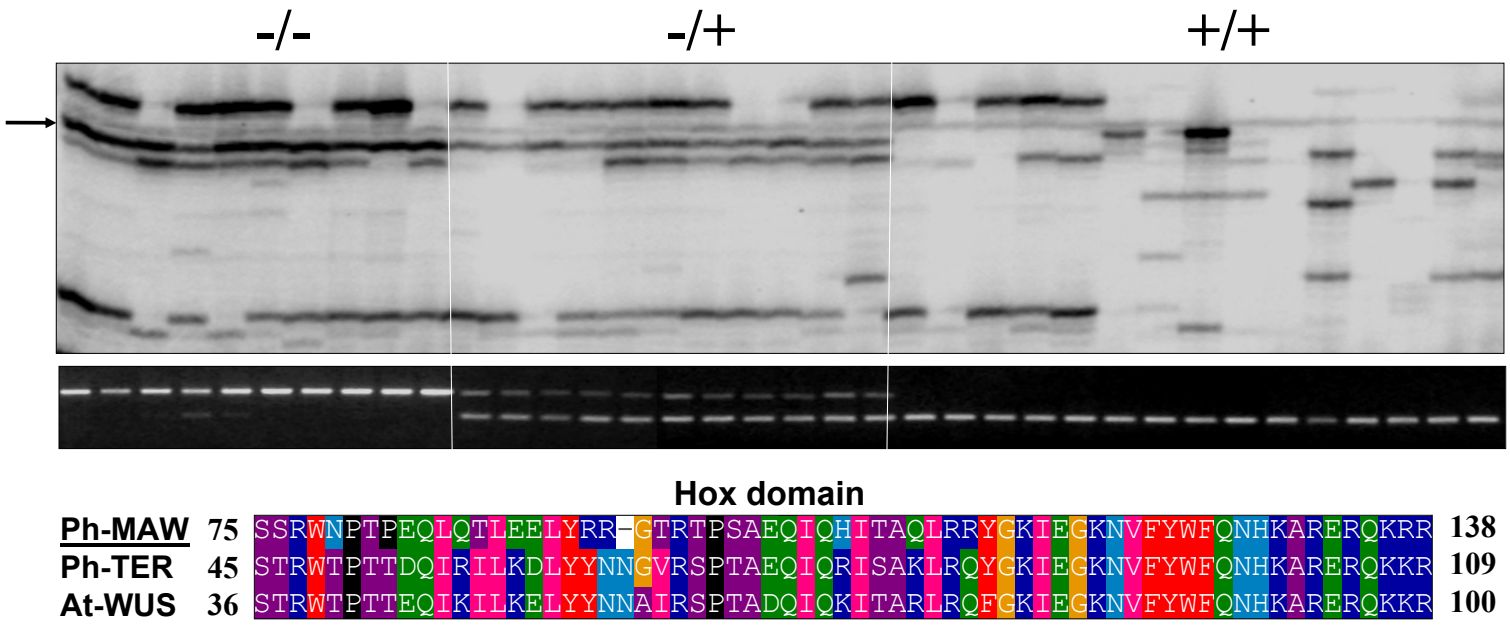

Fig. S1: Cloning of the *MAW* locus by Transposon Display. The upper panel shows part of a transposon display gel image with transposon flanking sequences amplified from a segregating family. Genotypes are indicated above the gel image. The arrow indicates a transposon flanking fragment present in all homozygous mutants and heterozygotes and absent in all homozygous wild-types. The bottom panel shows the result of a PCR with two gene specific primers flanking the transposon insertion in *MAW* (*maw*-1 allele). Numbers flanking the alignment of the hox region indicate # amino acids after the start codon.

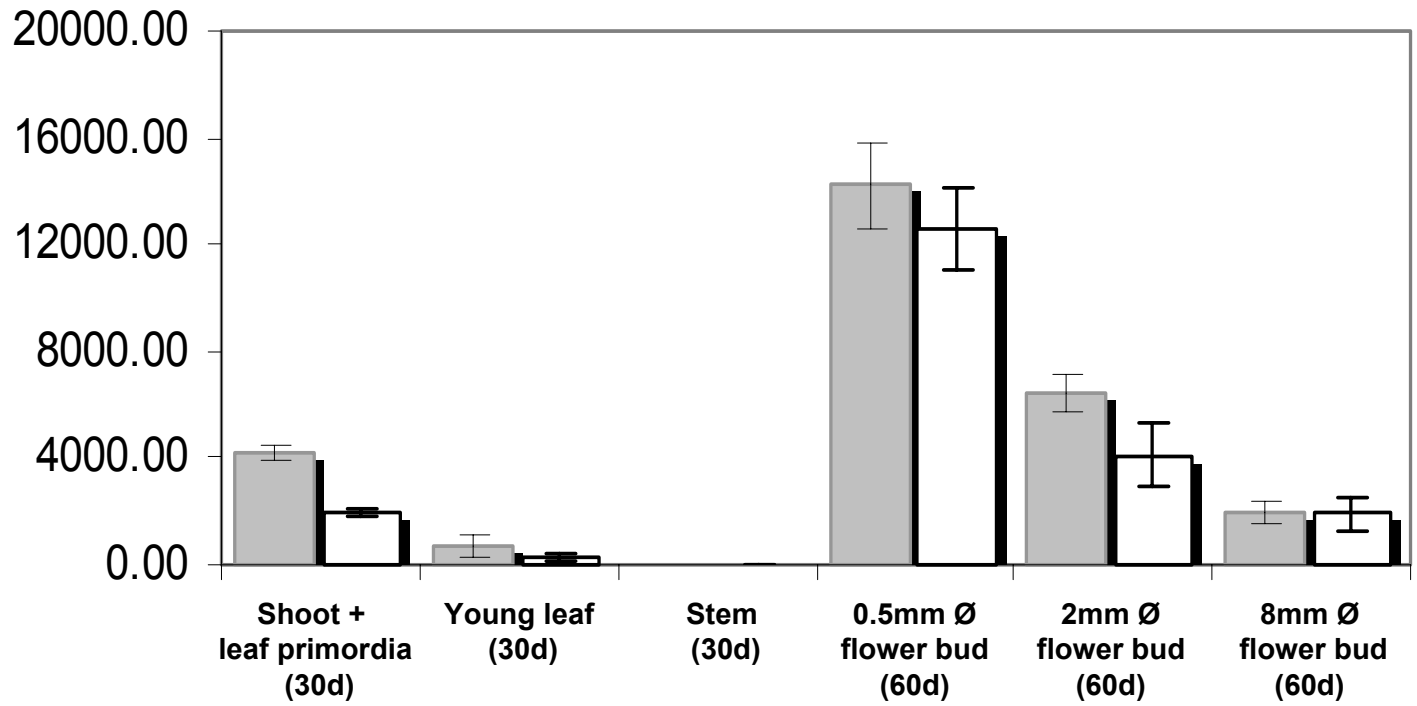

Fig. S2: *MAW* expression analysis by qRT-PCR. The y-axis shows x-fold expression with respect to the lowest encountered value set to one. Error bars represent standard deviation of three independent PCR experiments. Grey and white bars represent biological replicates. Tissue types are indicated below. Numbers between brackets indicate plant age in days after sowing.

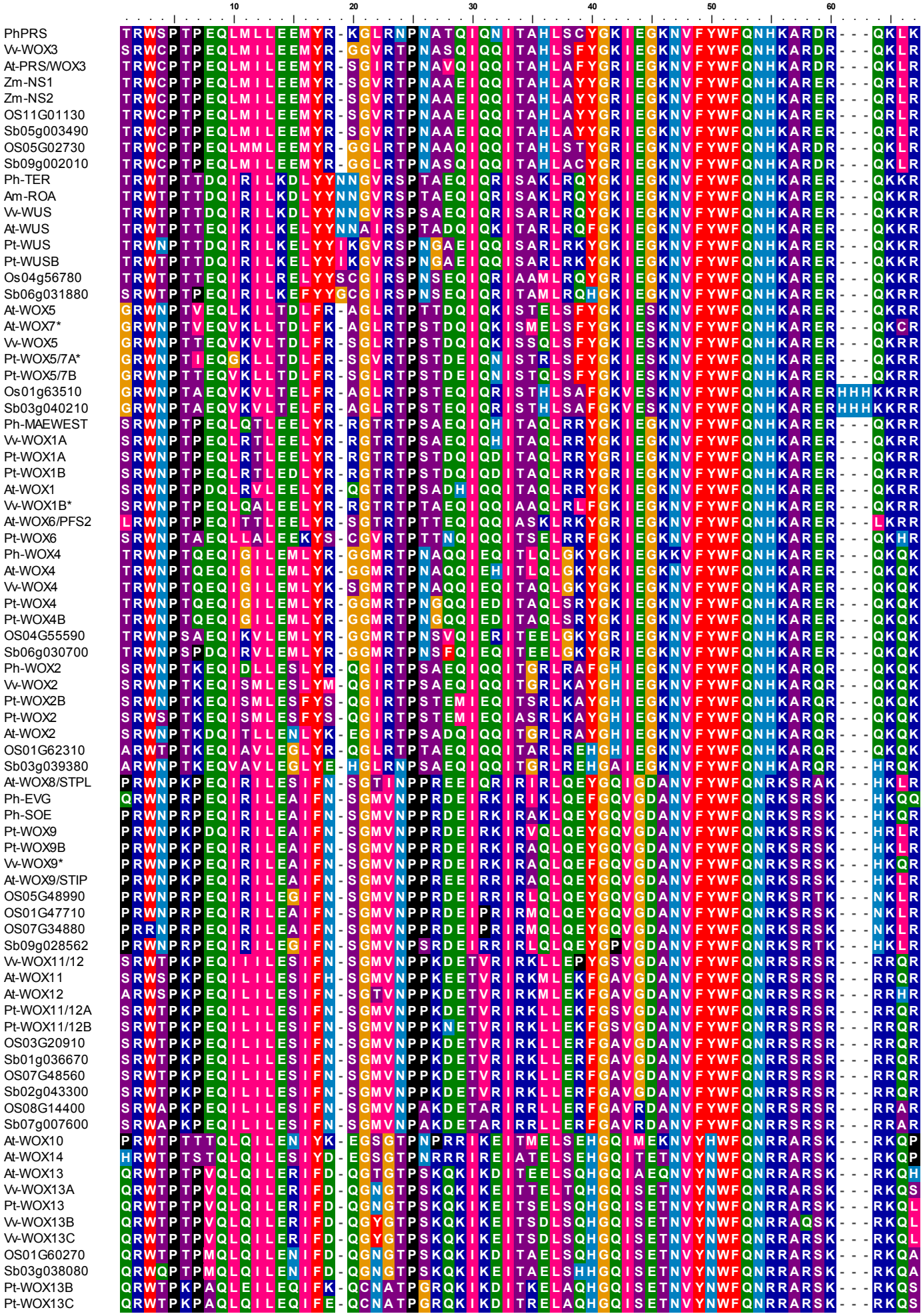

Fig. S3: **Alignment of the homeodomain region used for the construction of the NJ-Tree.**

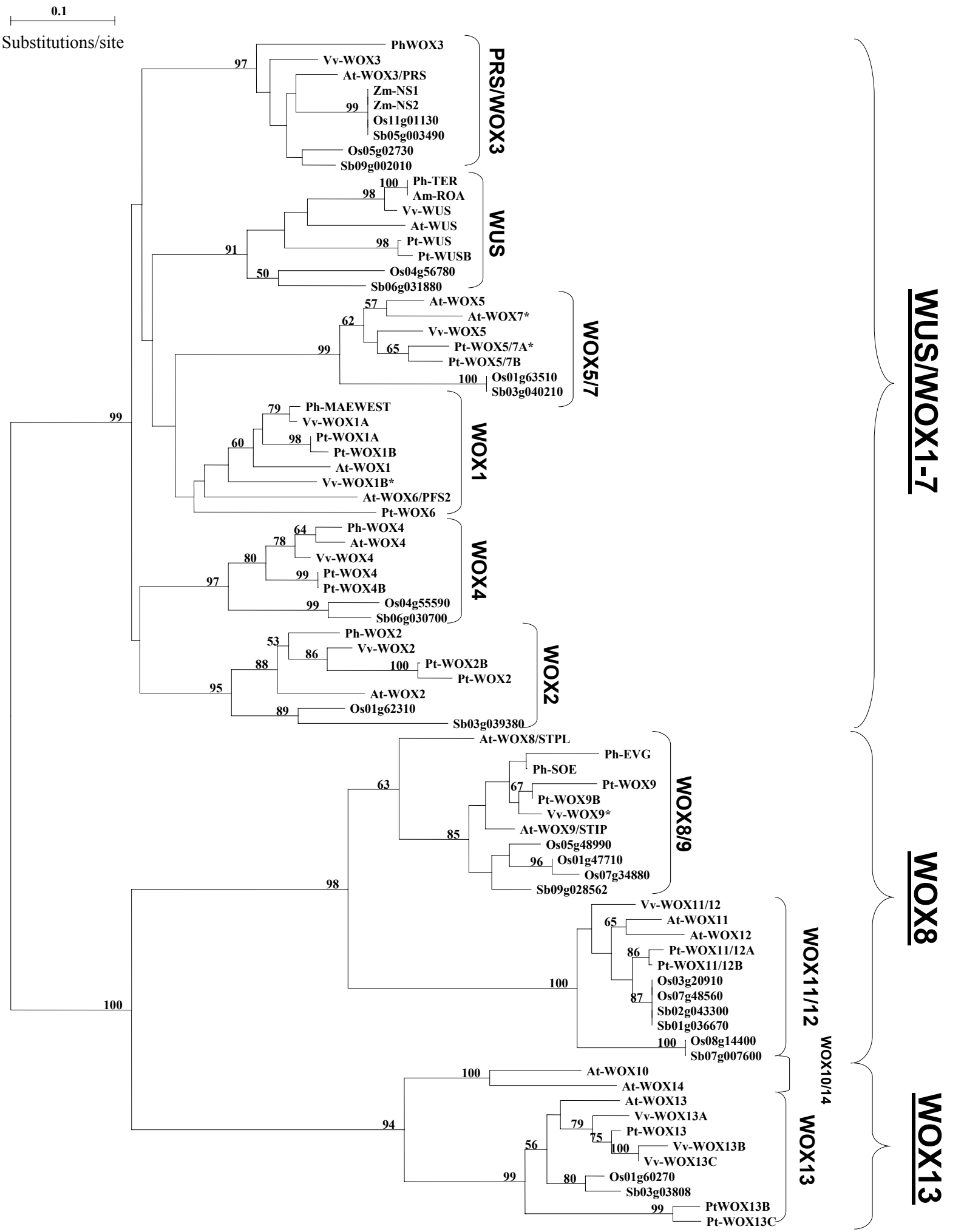

Fig. S4: Full NJ tree of the WOX homeodomain family

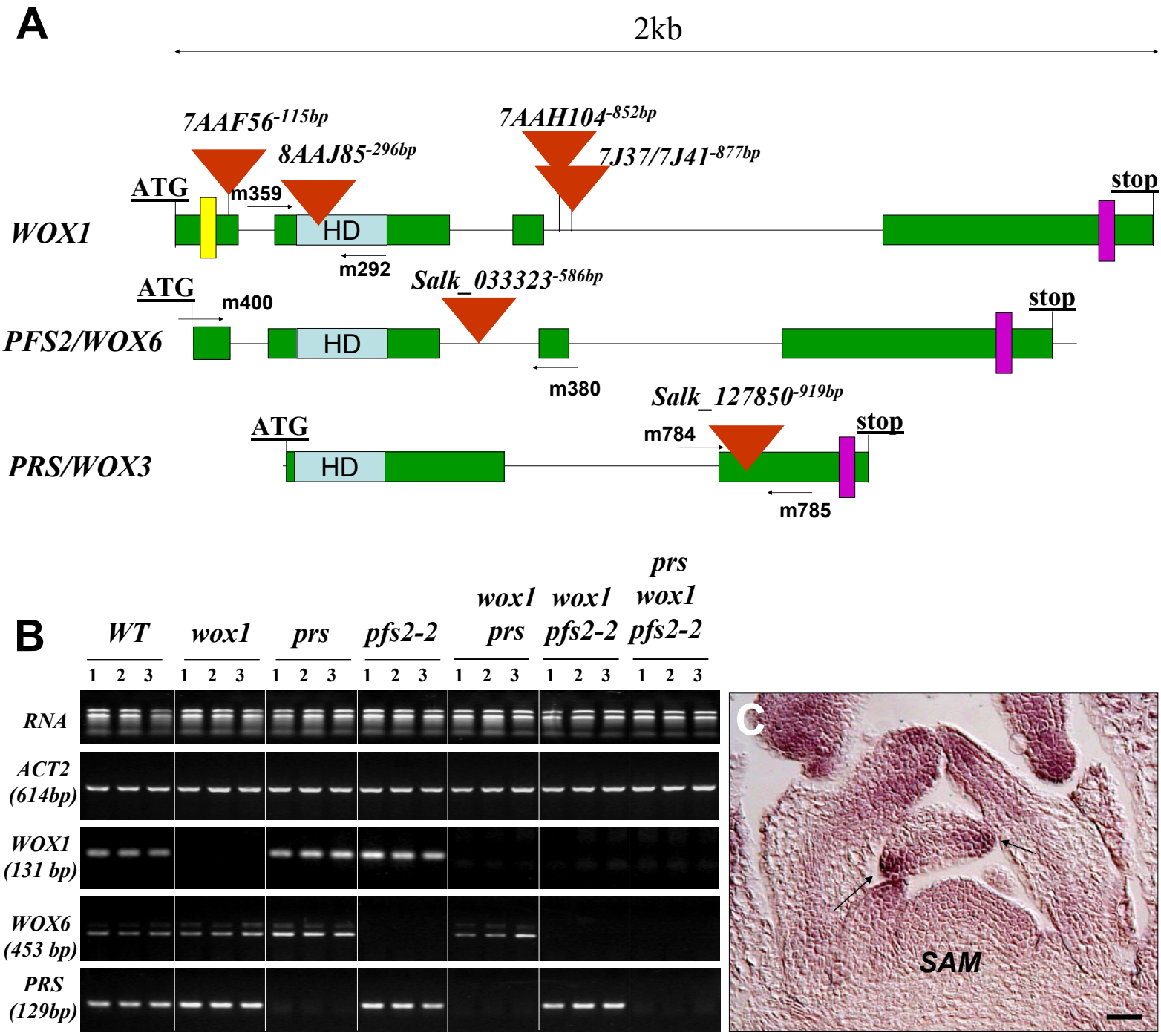

Fig. S5: A) Genomic structure and insert positions of Arabidopsis En1 transposon and T-DNA lines used in this study. Exact insert positions are indicated in superscript as number of basepairs downstream of the ATG in the genomic sequence. Exons are represented by green boxes from (ATG till stopcodon), and introns by black lines. HD: homeodomain region. Yellow and purple boxes indicate position of the 5' WOX1/4 box and the 3' WUS box respectively (see also Figure 3). **B) *WOX* gene expression analysis in WT and mutant lines by RT-PCR**. Genotypes are indicated above the gel images: *wox1* line: (8AAJ85); *wox6*: *pfs2-2* line: (SALK_033323); *prs* line: (SALK_127850) and double and triple combinations thereof. Lanes 1-3 for each genotype represent samples from three different individuals (independent biological replicates). The upper panel shows integrity of the inflorescence RNA samples used to prepare the cDNA templates. Expression of *ACTIN* (*ACT2*) was used as a positive control for cDNA synthesis (25 cycles). Positions of the *wox1*, *wox6* and *prs* insertion flanking primers (Table S1) used in the RT-experiment (35 cycles) are shown in fig. S5A. **C) *In situ* localization of Arabidopsis *WOX1* transcripts in developing leaves.** Longitudinal sections of the shoot apical meristem (SAM) and leaf primordia were hybridized with a digoxigenin-labeled antisense *WOX1* RNA probe (red staining). Arrows indicate a cross-section through a young leaf primordium with highest WOX1 expression detected in the margins, and lower levels in the central region across the leaf primordium. In the longitudinal leaf sections flanking the SAM, highest *WOX1* levels are detected distally. Sizebar = 10 µm

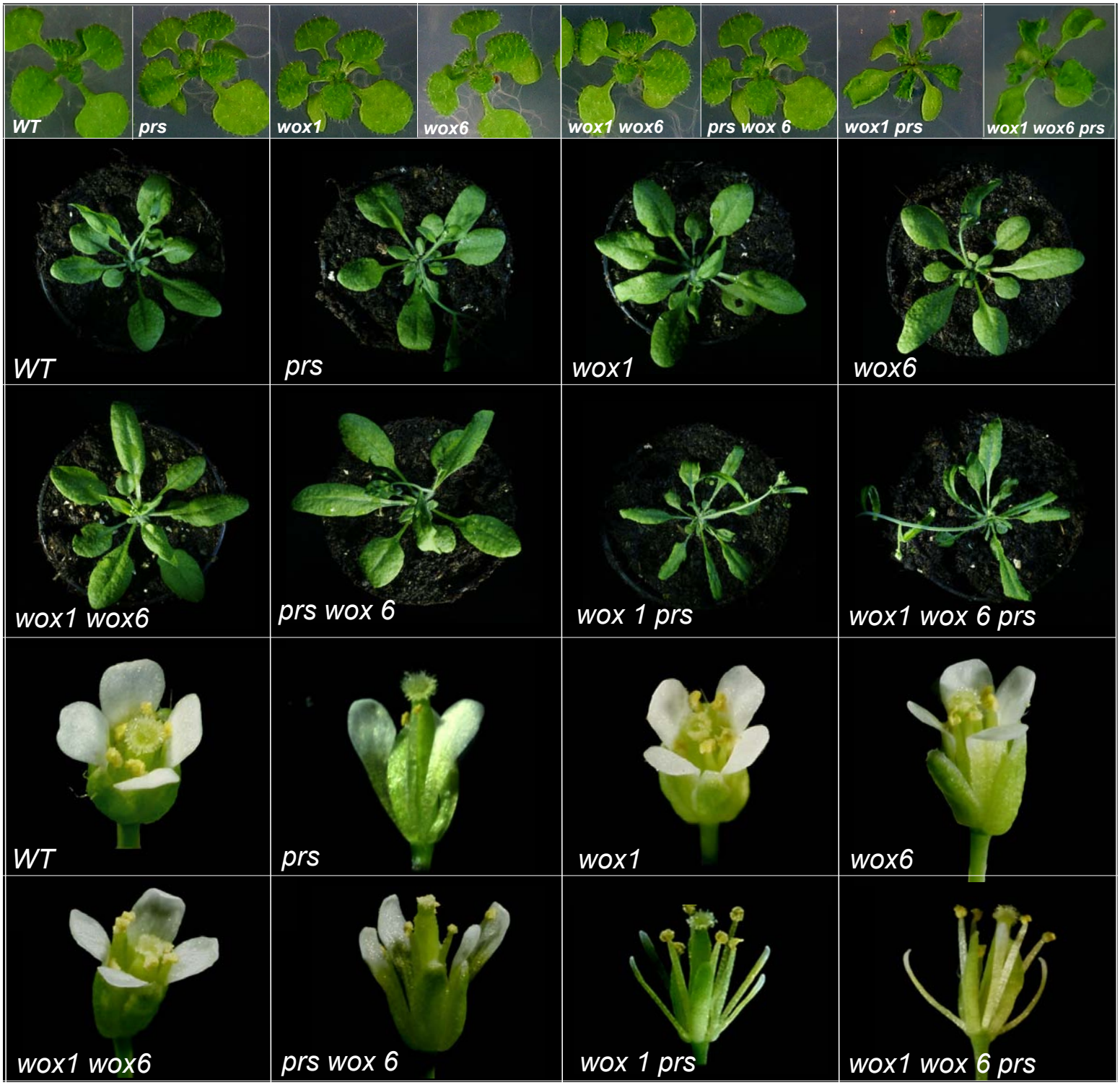

Fig. S6: Overview of all *Arabidopsis* phenotypes obtained in this study, showing seedlings, rosette stages at the onset of flowering, and individual flowers. Genotypes are indicated in italic below the images.